SAGE III Algorithm Theoretical Basis Document (ATBD)
Cloud Data Products

Compiled by the SAGE III ATBD Team

LaRC 475-00-106
Version 2.1
26 March 2002

Frontispiece: *View of the Earth's limb, as seen from Space Shuttle, showing cloud formations and the stratospheric aerosol layer. The picture is taken over Bolivia, looking east towards Brazil, during the period following the eruption of Mt Pinatubo in 1991.*

Abstract

The Stratospheric Aerosol and Gas Experiment (SAGE) III is the latest in a series of solar occultation satellite instruments designed for the measurement of stratospheric aerosols and gases. It will be making measurements of the extinction due to aerosols and gases at many wavelengths between 290 and 1550 nm. At least nine of these wavelengths have been designated as primarily for aerosol measurement. In the troposphere and winter polar stratosphere extinction will also occur in these and other channels, due to the presence of cloud along the optical path from the sun to the satellite instrument. Experience gained with its predecessor, SAGE II, has shown that intercomparison of the extinction at two or more wavelengths may be used to separate the effects of aerosol and cloud. This document describes the algorithm that will be used in conjunction with data from the SAGE III instrument to identify the presence of cloud along the optical path. The input data will consist of profiles of inverted extinction for three of the aerosol channels (525, 1020 and 1550 nm), with a vertical resolution of 0.5 km. The theoretical background to the algorithm is described, as are the results of simulation studies. These studies show that the algorithm may be expected to work well when aerosol sizes are small, but can give ambiguous results when larger aerosols are present, such as occurs as a result of a substantial volcanic eruption or close to the Earth's surface. The present algorithm, which will identify the presence of Type 2 polar stratospheric clouds as well as tropospheric clouds, is confined to altitudes between 6 and 30 km. In addition to describing and providing the theoretical background to the algorithm, this document also outlines the need for cloud presence determination, the SAGE III instrument, and its mode of operation. It also describes the input and output data sets, and suggests procedures for testing the algorithm, controlling data quality, and for validating the

output product. Details of the inversion procedure used to convert the raw SAGE III signal into vertical profiles of aerosol (and cloud where present), used as input to the cloud presence determination algorithm, are given in the SAGE III Aerosol Algorithm Theoretical Basis Document.

TABLE OF CONTENTS

CHANGE RECORD PAGE

ISSUE	DATE	PAGES AFFECTED	DESCRIPTION
Baseline	November 10, 2000	All	Supersedes: 1) SAGE III Cloud Theoretical Basis Document, LaRC 475-00-106, Release 1.2, dated February 18, 2000.
Version 2.1	March 26, 2002	Section 1.5; p. 3 Table 1.6.1; p.5	Added contributing authors Removed references to mixing ratio profiles

1.0 Introduction

The Stratospheric Aerosol and Gas Experiment III (SAGE III) is a critical part of the Mission to Planet Earth (EOS) Earth Observing System (EOS) program and contributes directly to the major goals identified in the March 1996 EOS Strategic Enterprise Plan 1996-2002. The EOS mission is to develop an understanding of the total Earth system and the effects of natural and human-induced changes on the global environment. SAGE III provides limb occultation measurements with a flexible instrument design that permits on orbit reprogramming and channel selection with up to 809 channels spanning the ultraviolet, visible, and near infrared (290-1550 nm). Solar observations will provide high resolution vertical profiles of multi-wavelength aerosol extinction, the molecular density of ozone, nitrogen dioxide, and water vapor, as well as profiles of temperature, pressure, and cloud presence. In addition, the inclusion of a repositionable solar attenuator will allow lunar occultation observations which will improve the geographic coverage and permit measurements of nitrogen trioxide and chlorine dioxide in addition to ozone, nitrogen dioxide, water vapor, and pressure.

1.1   Purpose

This Algorithm Theoretical Basis Document (ATBD) describes the algorithm used to identify the presence of cloud in the SAGE III data product. The algorithm and the document differ in nature from companion documents developed for the other SAGE III data products. The inversion schemes used by the algorithms described in these other documents utilize the raw radiometric data as input. The cloud presence determination scheme, in contrast, uses part of the output data derived by the aerosol algorithm described in the Solar and Lunar ATBD. Although cloud presence is a primary data product there are stronger similarities in its method with those used to derive the higher level data products, rather than with those for the other primary data products. The determination of cloud presence will nevertheless be carried out as part of the routine, event by event, processing of SAGE III data, to be initiated immediately after launch along with that for the other primary data products. The purpose of this document is to supply sufficient information about the algorithm for the corresponding code to be written, to justify the choice of algorithm, and to indicate how quality control and data validation may be carried out. Because of the resemblance of the determination of cloud presence to a higher level data product, the algorithm is much simpler than that for other primary products. In contrast, the problems of assessing errors in the data product, and of validating the data, present more challenges than occur with the other primary data products.

1.2   Scope

This document covers the algorithm from the accessing of the input aerosol data products to the output of the cloud presence profiles and the associated error assessment. Although a description of the instrument, the measurement geometry and an outline of the data handling is included, no attempt is made to describe the inversion from the radiometric data to the aerosol product. This is given in the Solar and Lunar ATBD, to which reference may be made. Apart from this omission, this cloud presence ATBD is a stand-alone document describing all features of the algorithm and its justification. The proposed method for the determination of cloud presence is original, although based on experience gained from analysis of SAGE II data. It depends upon the variation of extinction with wavelength for cloud being different from that for aerosol over the range of SAGE III wavelengths. As the method is new and as yet unused on actual data, space is given to a discussion of the reasons for the choice of this method, as compared to alternatives, and to a description of the results of simulation studies.

In its present form this is a living document, subject to change and development. Procedures for quality control require better specification and the validation program requires detailed definition. It is anticipated that these improvements will be made prior to launch. The present algorithm is limited to altitudes above 6 km and the emphasis is upon upper tropospheric clouds. Because of the horizontal viewing geometry of SAGE II, even quite thin cloud can cause the transmitted radiation received at the satellite to fall below the instrument threshold. Such cut-off altitudes will be recorded as cloud, but no data will be available from lower altitudes. Much of the cloud seen by SAGE III will fall into the subvisual category, and the instrument will be particularly suitable for the study of such cloud. Polar stratospheric clouds will also be identified where these occur and where they consist of particles large enough to show distinctive wavelength dependence in extinction (Type 2). Type 1 PSCs will give ambiguous signatures when queried by the presently proposed algorithm, and their routine identification and resolution requires further investigation.

Some assumptions are incorporated into the algorithm. Of these, the most significant is the assumption of horizontal homogeneity. SAGE III data products, including extinction, are inverted on the assumption that the atmosphere is spherically stratified in the region of the measurement. This assumption is valid for the stratosphere but is clearly untrue for most forms of cloud. Both the present algorithm and that previously used with SAGE II data use standard extinction data as input. For future algorithm developments to take cloud inhomogeneity into account, it may be necessary to use as input more fundamental SAGE III data, such as the atmospheric transmission found for individual scans across the solar disk. Other assumptions are that cloud shows little variation of extinction with wavelength, as opposed to that of the surrounding aerosol, and that the extinction at all10 wavelengths used in the algorithm is due to particulate matter only.

The present algorithm uses extinction data at three wavelengths, 521, 1020 and 1540 nm. The first two wavelengths are those used for SAGE II cloud studies, while the third has been added to improve the resolution of cloud from large aerosol particles. Aerosol extinction data will also be available at other wavelengths between 521 and 1020 nm (670, 758, and 869 nm) and consideration should be given at a later stage to the use of

data at these wavelengths in addition to, or in place of, that at 521 nm. Use of these wavelengths in future versions of the algorithm may also allow the determination of cloud presence to be taken to altitudes below 6 km.

Although cloud presence is determined after inversion for other data products, possible feedbacks may need to be considered. Use is often made of the aerosol data to produce long-term aerosol climatologies. Aerosol data must be screened for cloud presence before such analyses are made. More fundamentally, the presence of cloud may affect the inversion for other data products, either at the cloud altitude or lower. The degree to which these inversions may be influenced by cloud presence is most suitably determined by simulations that include cloud. These simulations should, if possible, take due account of the inhomogeneous nature of the cloud field.

1.3   Applicable Documents

1.3.1   Controlling Documents

EOS Science Plan, NASA HQ EOS, January 1999.

Mission to Planet Earth Strategic Enterprise Plan 1996-2002, NASA HQ EOS, May 1996.

Execution Phase Project Plan for Earth Observing System (EOS), GSFC 170-01-01, Rev. A., May 1995.

1.3.2   SAGE III ATDB Reference Documents

SAGE III Algorithm Theoretical Basis Document: Transmission Data Products, LaRC 475-00-108, November 2000.

SAGE III Algorithm Theoretical Basis Document: Cloud Presence Data Products, LaRC 475-00-106, November 2000.

SAGE III Algorithm Theoretical Basis Document Solar and Lunar Algorithm, LaRC 475-00-109, November 2000.

1.4   Revision History

The original version of this document was dated November 15, 1996. Version 1.1 was released on 15 April 1997. Version 1.2, was released on 18 February 2000. Version 2.0 was released on 10 November 2000. This release, version 2.1, is dated March 2002.

1.5 Contributing Authors

The SAGE III ATBDs were drafted by a team of SAGE III science team members and SAGE III science cadre, led by one of the science team members. The entire team participated in oral and written revisions of the methodology and documentation as part of the SAGE III science team meetings and research activities.

Contributing Authors	Affiliation
Colette Brogniez	University de Lille, France
Er-Woon Chiou	SAIC
William P. Chu	NASA Langley Research Center
Albert A. Chernikov	Central Aerological Observatory
Derek M. Cunnold	Georgia Tech
John DeLuisi	NOAA
Philip A. Durkee	Naval Postgraduate School
Nikolai F. Elansky	Russian Academy of Science
Benjamin M. Herman	University of Arizona
Peter V. Hobbs	University of Washington
Geoff S. Kent	Science and Technology Corporation
Jacqueline Lenoble	University de Lille, France
M. P. McCormick, Principal Investigator	Hampton University
Hope A. Michelsen	AER
Alvin J. Miller	NOAA/NCEPS
Volker Mohnen	State University of New York at Albany
Randy Moore	SAIC
Michael C. Pitts	NASA Langley Research Center
Lamont R. Poole	NASA Langley Research Center
Venkatachalam Ramaswamy	Princeton University
David Rind	Goddard Institute for Space Studies
David Risley	SAIC
Michael W. Rowland	SAIC
Philip B. Russell	NASA Ames Research Center
Vinod K. Saxena	North Carolina State University
Eric P. Shettle	Naval Research Laboratory
Victor E. Sothcott	SAIC
Ghassan Taha	University of Arizona
Larry W. Thomason	NASA Langley Research Center
Charles R. Trepte	NASA Langley Research Center
Gabor Vali	University of Wyoming
Lelia B. Vann	NASA Langley Research Center
Robert E. Veiga	SAIC
Pi-Huan Wang	Science and Technology Corporation
Steven C. Wofsy	Harvard University
David C. Woods	NASA Langley Research Center

Joseph M. Zawodny	NASA Langley Research Center

1.6 SAGE III Standard Data Products

Table 1.6.1 SAGE III standard data products

PRODUCT NAME	UNCERTAINTY Systematic :: Precision	TEMPORAL RESOLUTION	HORIZONTAL Resolution :: Coverage	VERTICAL Resolution :: Coverage
Level 1B Transmission (≤80 wavelengths) Solar Events	0.05% :: 0.05%	1/(2 minutes), 30/day	<2 x <1 deg :: Global	0.5 km :: 0-100 km
Aerosol Extinction Stratospheric Optical Depth (at 9 wavelength bands), Aerosol to molecular/extinction ratio at 1020 nm (solar only)	5% :: 5%	1/(2 minutes), 30/day	<2 x <1 deg :: Global	0.5 km :: 0-40 km
O_3 Concentration Slant Path Col. Density	6% :: 5%	1/(2 minutes), 30/day	<2 x <1 deg :: Global	0.5 km :: 6-85 km 0.5 km :: 50-85 km
NO_2 Concentration Slant Path Col. Density	10% :: 15%	1/(2 minutes), 30/day	<2 x <1 deg :: Global	0.5 km :: 10-50 km 0.5 km :: 10-50 km
H_2O Concentration	10% :: 15%	1/(2 minutes), 30/day	<2 x <1 deg :: Global	0.5 km :: 0-50 km
NO_3 (Lunar Only) Concentration	10% :: 10%	1/(2 minutes), ≤30/day	<2 x <1 deg :: Global	0.5 km :: 20-55 km
OClO (Lunar Only) Concentration	25% :: 20%	1/(2 minutes), ≤30/day	<2 x <1 deg :: Global	0.5 km :: 15-25 km
Pressure	2% :: 2%	1/(2 minutes), 30/day	<2 x <1 deg :: Global	0.5 km :: 0-85 km 1000-0.004 hPa
Temperature Profile	2K :: 2K	1/(2 minutes), 30/day	<2 x <1 deg :: Global	0.5 km :: 0-85 km
Cloud Presence	N/A	1/(2 minutes), 30/day	<2 x <1 deg :: Global	0.5 km :: 6-30 km

2.0 Background

SAGE III is the fifth generation of solar occultation instruments designed to measure atmospheric aerosols and gaseous species in the atmosphere. The solar occultation method employs the attenuation of the Sun's rays as observed through the limb of the Earth's atmosphere to determine the vertical distribution of important atmospheric constituents. Measurements are made during each sunrise and sunset (an "event") encountered by the spacecraft (~30/day). This method is well suited for long-term monitoring of trends and variability in key species such as ozone since the instrument is recalibrated during each event. The instrument concept originated as a hand-held, single wavelength sunphotometer (Stratospheric Aerosol Measurement or SAM) which was flown onboard an Apollo mission in 1975 [Pepin and McCormick, 1976]. SAM II was a one wavelength (1000 nm) instrument which operated on Nimbus-7 between 1978 and 1994 [McCormick *et al*., 1979 and 1981]. The Stratospheric Aerosol and Gas Experiment (SAGE) operated on the Application Explorer Mission 2 (AEM-2) spacecraft between 1979 and 1981. This instrument made measurements at 4 wavelengths and measured molecular density profiles of O_3 and NO_2 in addition to aerosol extinction at 2 wavelengths (450 and 1000 nm) [McCormick *et al*., 1979]. SAGE II has operated on the Earth Radiation Budget Satellite (ERBS) since 1984 and makes measurements at 7 wavelengths. In addition to the species measured by SAGE, SAGE II measures the molecular density profile of H_2O and aerosol extinction at 4 wavelengths (385, 453, 525 and 1020 nm) [Mauldin *et al.,* 1985; McCormick, 1987]. In SAGE III, a charged coupled device (CCD) linear array provides spectral coverage from 280 to 1040 nm. In addition, a single photodiode adds aerosol extinction measurements at 1550 nm. [McCormick *et al*, 1991; Mauldin *et al*., 1989; McCormick *et al.,* 1993a]. A repositionable solar attenuator will permit both solar and lunar occultation measurements, increasing the geographical coverage and allowing for the detection of nitrogen trioxide and chlorine dioxide. The incorporation of the CCD array will permit the measurement of gaseous species from multichannel absorption signatures simplifying the retrieval process, and 16-bit digitization will improve the precision and altitude range of the measurements.

2.1   SAGE III Experimental Objectives

The science objectives to be accomplished by SAGE III are:

*   Retrieve global profiles of atmospheric aerosol extinction, temperature, pressure and molecular density profiles of ozone, water vapor, nitrogen dioxide, nitrogen trioxide, and chlorine dioxide with 0.5 km vertical resolution.

- Characterize tropospheric as well as stratospheric clouds and investigate their effects on the Earth's environment, including radiative, microphysical, and chemical interactions.

- Determine long-term trends in gaseous species and temperature.

- Provide atmospheric data essential for the interpretation and calibration of other satellite sensors, including EOS instruments.

- Investigate the spatial and temporal variability of these species in order to determine their role in climate processes, biogeochemical cycles, and the hydrological cycle.

2.2   Relevance of Cloud Measurements to EOS

Tropospheric Clouds

Clouds in the atmosphere are major determinants of the planet's solar and longwave energy balance and, thus, are important in governing Earth's climate. While the presence of low clouds leads to the reflection of a large amount of solar radiation, the presence of middle and high level clouds contribute to the "greenhouse" effect. The higher a cloud base and top are, the greater the infrared trapping of radiative energy and the tendency to warm the planet. Present-day satellite observations indicate that the presence of clouds overall has a tendency to cool the globe. Observations and model calculations suggest that the radiative heating of the atmosphere is critically dependent on the presence or the absence of condensed water (in liquid or solid form). Clouds are intimately linked to convection and the hydrologic cycle in the atmosphere. The role of water in all its phases is important for the amount of moisture entering the stratosphere from the troposphere across the tropical tropopause. Condensed water could also be playing a non-negligible role in the microphysical-chemical processes in the vicinity of the tropopause. A particular example in this regard is that of the polar stratospheric clouds (PSCs), which are now recognized to be important for heterogeneous chemical reactions that lead to ozone depletion.

As part of the hydrologic cycle, clouds are extremely significant in governing the feedbacks associated with climate change. Current concerns include uncertainties in the sign and magnitude of changes associated with clouds in response to the radiative forcing by the increasing concentrations of anthropogenic greenhouse gases and aerosols. Because of the climatic importance outlined above, there is a pressing need to identify the presence of clouds in the atmosphere and to quantify their physical properties. The principal factors that must be known in order to assess the role of clouds are the sizes and concentrations of the condensates, their optical characteristics, and their radiative interactions. A knowledge of these physical entities is useful and thus desirable in two respects: first, they are aids in the diagnostic interpretations of the linkages between cloud processes and other aspects of climate; second, such information is vital in evaluating the simulations of present-day weather and climate general circulation models

12

and in ascertaining their robustness [Wetherald *et al.*, 1991]. Thus, the information on clouds is relevant for present-day climate modeling and in leading to more reliable predictions of global climate change.

In the past, observation of the sun through the earth's limb in the solar spectrum has offered a wealth of information on clouds [Woodbury and McCormick, 1983, 1986]. Examples of such satellite systems are SAGE, SAGE II, and SAM II. Information from these satellites has yielded very useful information on the widespread presence of thin cirrus that cannot normally be detected by nadir-looking devices. Nadir looking detection devices have historically been unsuited to characterize these tenuous clouds. The SAGE III configuration goes beyond these original limb detection units and seeks to, by employing detection at multiple wavelengths, quantify the optical and the physical features of these condensates.

This series of solar occultation satellites is particularly useful for the detection and study of thin high cloud, often subvisual. These have widespread extent and, even though they are thin, their reflection of solar radiation and trapping of infrared radiation can be significant contributors to the atmospheric radiation budget. Further, the radiative heating due to cirrus clouds can be comparable to or even exceed that due to the other constituents in the upper tropospheric regions, thus becoming significant in the maintenance of the thermal profile in those regions [Ramanathan *et al.*, 1983; Ramaswamy and Ramanathan, 1989]. The detection of such clouds and inferences of their optical properties is thus a critical aspect in understanding quantitatively the role of clouds in the Earth's climate and for gauging any variations or changes from the present climate. SAGE III will also further establish a climatology of such clouds which has proved difficult to get from other platforms. Such climatology would also aid in the validation of cirrus cloud simulations by weather and climate general circulation models. Such validation is a critical element in enhancing the credibility of the GCMs. A third reason for the study of high tropospheric cloud is that the microphysical aspects concerning the hydrologic cycle in the upper troposphere are linked closely to the formation of the condensates that comprise cirrus clouds. Direct observations of such clouds and their properties would improve the understanding and simulation of the microphysical-hydrologic interactions [Detwiler and Ramaswamy, 1990]. This interaction is closely linked, in turn, to the radiative properties of the clouds.

Polar Stratospheric Clouds (PSCs)

Field missions and laboratory experiments over the past decade have firmly established that PSCs play a crucial role in the formation of the Antarctic ozone hole and in increasing the potential for significant springtime ozone losses in the Arctic. Heterogeneous chemical reactions occur quite readily on PSC particle surfaces, the most prominent one being the reaction between the benign chlorine reservoir compounds HCl and $ClONO_2$. This reaction releases Cl_2, which in the presence of sunlight is photolyzed to Cl atoms, which can readily destroy ozone. The surface heterogeneous reactions also sequester stratospheric odd nitrogen as non-reactive HNO_3, thus effectively preventing the re-formation of the chlorine reservoir compounds and further increasing the potential

for ozone destruction. There is a need for continuing PSC observations from space to refine climatologies established by earlier satellite measurements and to address existing uncertainties in the composition and reactive efficiency of Type 1 (HNO_3/H_2O) PSCs. Perhaps the most glaring area of uncertainty in polar ozone depletion is the denitrification process, or the process whereby odd nitrogen is irreversibly removed from the polar stratosphere. Multi-wavelength PSC observations coupled with improved temperature measurements (such as will be available from SAGE III) should provide useful information on the details of denitrification.

Impact on other SAGE III Data Products

Although cloud presence is determined as a data product in its own right, certain feedbacks can occur with respect to other SAGE III data products. The simplest of these is with the aerosol product from which the cloud presence is derived. Solar occultation data has been much used in the past to derive aerosol climatologies. In the stratosphere, polar stratospheric cloud and tropopause cloud represent contaminants that must be pre-screened before calculation of seasonal or long-term averages. In the troposphere, cloud at all altitudes will affect the data averages. Accurate determination of cloud presence is thus essential to these types of analysis.

More fundamentally, there exists some uncertainty as to the accuracy with which other SAGE III data products (e.g. water vapor, temperature etc.) may be measured in the presence of cloud. Cloud attenuates the signal received from the sun at all wavelengths, and its effects may have to be removed before inversion for the required data product. Present algorithms also assume that all atmospheric species have spherically homogeneous distributions in the vicinity of the tangent point; this is clearly not true for cloud. One possible course of action (the simplest) is to reject all cloud contaminated data; another is to carry out simulations to determine the likely effects of cloud on inversion for other products. These simulations should take due account of the inhomogeneous nature of the cloud field.

2.3   Historical Perspective and Heritage

Tropospheric Aerosol and Cloud Measurements

SAGE III is the latest in a series of solar occultation satellite instruments designed to measure stratospheric and upper tropospheric aerosols and gases [McCormick *et al*., 1991]. This instrument and its predecessors (SAM II, SAGE, and SAGE II) form a series of increasingly more complex and powerful instruments which carry out these measurements using the same basic principle. Although they were not designed for tropospheric measurement it has been found possible to extend the retrieval of data from these previous instruments down to the upper troposphere. In particular the data obtained in the aerosol channels, notably that at 1000 nm (SAGE) and 1020 nm (SAGE II) has been used to derive information about the distribution of high altitude cloud. The earlier cloud climatologies that were developed [Woodbury and McCormick, 1983, 1986; Chiou

et al., 1990] relied on the fact that the extinction due to cloud was likely to be much greater than that due to aerosol. An arbitrary extinction level was set and all extinction values greater than this level were attributed to cloud. Although useful information was obtained about the global distribution of thin high cloud by these methods, problems were encountered at certain latitudes and times due to the fact that the aerosol extinction was variable and could on occasion be above the discrimination level chosen. The cloud distributions obtained from these analyses were compared with those obtained by other workers using different instruments [Hahn *et al*. 1982; Barton 1983; Stowe *et al*. 1989]. With respect to the locations of the regions of maximum cirrus occurrence, the relative importance of these regions, and the seasonal variations, good agreement was found.

An alternative method of separating aerosol and cloud using SAGE II extinction data at two wavelengths, 1020 and 525 nm, has been described by Kent and McCormick [1991] and Kent *et al*. [1993]. The extinction produced by cloud particles is approximately equal at the two wavelengths, whereas the aerosol extinction is normally wavelength dependent. This difference in wavelength behaviour is used to separate the two components. In the second paper, Kent *et al*. [1997a] also described the validation of their model using data obtained by airborne lidar at the same time, and in the same atmospheric volume, as the SAGE II measurement. This comparison has enabled SAGE II cloud measurements to be interpreted in terms of the visual characteristics of the cloud. By virtue of the long horizontal path over which SAGE II makes its measurements, the extinction is extremely sensitive to the presence of thin cloud. Comparison of the SAGE II data with the concurrent lidar data, and interpretation of the latter in visual terms, has shown that much of the SAGE II cloud data corresponds to subvisual cirrus, and that the lowest extinction levels measurable are about one order of magnitude below those produced by cloud at the subvisual-visual threshold. Sassen *et al*. [1989] and Sassen and Cho [1992] described measurements made on subvisual cirrus clouds (optical thickness less than 0.03), similar to those viewed by SAGE II. Such optically thin clouds are not readily distinguished by satellite imagery, particularly against a bright background, but their presence and characteristics may be studied with lidar. The frequency of occurrence of cirrus cloud as viewed by SAGE and SAGE II has always been higher than that viewed by other instruments; the average occurrence viewed by the SAGE instruments over the tropics is between 50% and 75%. Liao *et al*. [1995a] have interpreted this difference as due to the relatively small horizontal cloud size (~75 km) as compared to the SAGE II optical path (~200 km). SAGE II possesses a vertical resolution of 1 km in its inverted data product, determinable from observations of the sun and the orbital geometry, and is not dependent on the estimation of cloudtop pressure altitude. Disadvantages of the SAGE II technique include a relatively low sampling rate (twice per orbit) and poor horizontal resolution on each measurement (~200 km). Successive measurements are also widely separated geographically, so patterns of cloud distribution in a given region may only be found by accumulating data over a considerable period of time. In many of these features the SAGE II data may be regarded as complementary to those from nadir measurements.

The method for separating cloud and aerosol used by Kent *et al*. [1993] [which will be referred to as the slope/intercept method] requires two input parameters that are

determined from an extended aerosol / cloud data set. As a step in the establishment of an aerosol / cloud data base, this has been carried out in terms of three-month time segments, one kilometer height intervals, and 20° latitude bands. Since these parameters are determined from an extended data set around the time of each event to be classified, the method cannot be applied immediately to a current measurement. The slope/intercept method is not the only method that has been tried. Wang *et al*. [1994] have used the ratio of the extinction at 525 nm to that at 1020 nm to distinguish aerosol from cloud (this will be referred to as the slope method). This method is similar to the slope/intercept method but somewhat simpler, requiring only one input parameter. The slope method may require this parameter to be derived from segments of the data ensemble, as in the slope and intercept method, or it may use a fixed value. Other methods have also been tried, based on cluster analysis (Chiou, 1995, private communication), and on the presence of strong gradients in the aerosol extinction profile (Veiga, 1995, private communication). They have not been extensively used but may merit further exploration, particularly under conditions where the more standard methods cannot be used.

Global maps of SAGE II tropospheric cloud distribution are currently available on the NASA Langley Research Center's Atmospheric Science Data Center (ASDC) (formerly the Langley Research Center Distributed Active Archive Center). Individual maps show the cloud distribution averaged over three month time intervals from 1984 to 1991. They extend from 8.5 km to 19.5 km altitude with a vertical resolution of 1 km. The cloud data used to produce the maps for the Langley ASDC has been derived from the SAGE II 1020 and 525 nm aerosol extinction data using a modified version of the slope / intercept method discussed above. The slope / intercept method and alternative methods of separating aerosol from cloud do not work well at times of recent volcanic activity. Aerosols resulting from volcanic gases injected into the stratosphere are significantly larger than background aerosols, they show little or no variation of extinction with wavelength and are not readily distinguished from cloud using the SAGE II wavelengths. No cloud data following the eruption of Mt. Pinatubo in June, 1991 has yet been put into the Langley ASDC although the stratosphere has now returned to close enough to a background state for this to be resumed. The data in the Langley ASDC does not extend to altitudes below 6 km, as data is then only available at the 1020 nm wavelength. We may note, however, that, at lower altitudes, large aerosols similar in size to those of recent volcanic origin will be present. These are likely to make uncertain any aerosol/cloud separation method that is based on the wavelength characteristics of the aerosol optical properties.

A number of publications exist that report climatologies and other studies based on the SAGE and SAGE II high cloud measurements. The earliest climatologies were presented in terms of the SAGE total cloud amount integrated over an altitude range several kilometers thick near the tropopause [Woodbury and McCormick, 1983, 1986]. These studies were primarily concerned with the geographical distribution of cloud occurrence frequency and statistical intercomparison with other published cloud climatologies. Somewhat more recently Chiou *et al.,* [1990] have reported similar statistics for SAGE II, including seasonal changes and sunrise-sunset differences. Kent *et al*., [1994] have examined SAGE II cloud data with a vertical resolution of 1 km, showing the variation of

tropical high cloud amount with altitude and reported the existence of an ENSO effect in the occurrence of tropical high cloud. This analysis has been carried a step further by Kent *et al.,* [1995] where the high cloud amount in the tropics is related to changes in the underlying surface temperature. Wang *et al*., [1994] discuss the relationship of SAGE II tropical cloud data to the ambient temperature and the possible deduction of information on particle growth processes. Wang *et al*. [1995] have extended the cloud analysis to lower altitudes and shown how bounding limits may be placed on the actual cloud frequencies deduced for such altitudes. Liao *et al*. [1995a, 1995b] have made a detailed comparison between the SAGE II data sets and high level clouds as obtained by the International Satellite Cloud Climatology Project (ISCCP). Their aim has been to reconcile the different cloud occurrence frequencies as seen by the two data sets and the difference in cloudtop altitudes.

Polar Stratospheric Cloud Measurements

Some 300 visual sightings of stratospheric mother-of-pearl clouds were recorded in the Arctic and Antarctic during the century from 1870 to 1970 [Stanford and Davis, 1974]. The dawning of the age of spaceborne remote sensing demonstrated, however, that high-latitude stratospheric clouds occurred much more frequently than this. Analysis of aerosol extinction profiles obtained during the early operational phase (1978-79) of SAM II showed recurrent layers of enhanced extinction at stratospheric altitudes during both polar winters [McCormick *et al*., 1982]. The enhanced extinction events were given the generic name polar stratospheric clouds (PSCs) and were found to be highly correlated with cold synoptic-scale temperatures (<200 K). Later studies of the SAM II data record [McCormick and Trepte, 1986; 1987a] confirmed that the clouds are common features in the lower winter stratosphere (below 25 km) of both polar regions. More recently, Poole and Pitts [1994] used SAM II data from 1978-1989 to study the long-term probability of PSC occurrence. They showed that Antarctic PSCs are typically observed by SAM II from mid-May to early November (with a peak probability of about 0.6 in August), while the typical Arctic PSC season extends from late November to early March (with a peak probability near 0.1 in early February). Poole and Pitts found that maximum PSC sighting probabilities in both polar regions occur in the longitude region from 90°W through the Greenwich meridian to 90°E, where temperatures are coldest on average. They also showed that temperatures required for Antarctic PSC formation are much colder in September than June, a pattern consistent with the irreversible loss of HNO_3 and H_2O vapor in sedimenting PSC particles.

The method of identifying PSCs in the SAM II data set differs from that used for tropospheric cloud in the SAGE II data set. The latter method compares the extinctions measured at two wavelengths (525 and 1020 nm). Since SAM II measured aerosol extinction at only one wavelength (1000 nm), Poole and Pitts used a "threshold" PSC identification scheme which differs fundamentally from both the SAGE II method and the multi-wavelength approach outlined later in this document for use with the SAGE III data set. The SAM II database was searched *ex post facto* by altitude over 10-day periods to identify measurement events with both cold temperature and an extinction ratio (the ratio of total extinction to molecular extinction) significantly larger than that of the local

background sulfate aerosol. For each 10-day period, a background aerosol profile was defined as the median of all extinction ratio measurements having collocated temperatures above 200 K. Then a measurement was classified as a PSC if the collocated temperature was below 200 K and the local extinction ratio minus its uncertainty was greater than the appropriate background value plus 3 times its median deviation.

Polar Mesospheric Cloud Measurements

The characteristics of Polar Mesospheric Clouds (PMCs), have been reviewed by Thomas [1989] and by Gadsen and Schröder, [1989]. They occur near the mesopause, (at an altitude of 80 to 85 km), in each summer polar region at latitudes poleward of about 55°. They are generally observed during an approximately twelve week period centered two weeks after the summer solstice, [Olivero and Thomas, 1986; Thomas and Olivero, 1989]. Satellite observations have been reported from scattered light observed by OGO 6 [Donahue *et al.*, 1972] and by the Solar Mesospheric Explorer (SME) satellite, [Olivero and Thomas, 1986; Thomas and Olivero, 1989]. They are believed to consist of small ice particles formed at or below the summer mesopause (near 90 km), where the temperatures can go below 140 K.

Recently Debrestian *et al.* [1996] and Shettle *et al.* [1995] have reported on the observations of PMCs from another solar occultation instrument, POAM II (Polar Ozone and Aerosol Measurement). The strongest PMC that they reported had a slant optical depth of 0.01 (at a wavelength of 442 nm), with the weakest PMC being limited by their signal-to-noise to an optical depth of 0.0005 along their tangent line of sight. These correspond to the brightest of the SME observations, which cover 2.5 orders of magnitude or twice the range of the POAM II observations. The POAM observations exhibited a strong wavelength dependence, usually only detecting the cloud layers at their shortest wavelengths (353 to 600 nm). This is consistent with the small particle sizes inferred from the SME data of mean radius of 43±16 nm, with all cases smaller than 100 nm [Rusch *et al.*, 1991].

The characteristics of Polar Mesospheric Clouds (PMCs), have been Reviewed by Thomas [1989] and by Gadsen and Schröder, [1989]. They occur near the mesopause, (at an altitude of 80 to 85 km), in each summer polar region at latitudes poleward of about 55°. They are generally observed during an approximately twelve week period centered two weeks after the summer solstice, [Olivero and Thomas, 1986; Thomas and Olivero, 1989]. Satellite observations have been reported from scattered light observed by OGO 6 [Donahue *et al.*, 1972] and by the Solar Mesospheric Explorer (SME) satellite, [Olivero and Thomas, 1986; Thomas and Olivero, 1989]. They are believed to consist of small ice particles formed at or below the summer mesopause (near 90 km), where the temperatures can go below 140 K. Debrestian *et al.* [1997a and 1997b] and Shettle *et al.,* [1995] have reported on the observations of PMCs from another solar occultation instrument, POAM II (Polar Ozone and Aerosol Measurement). The POAM observations exhibited strong wavelength dependence, usually only detecting the cloud layers at their shortest wavelengths (353 to 600 nm). Debrestian *et al.* [1997a] have used this wavelength dependence to derive particle sizes for the PMCs of 20 to 70 nm. This is

consistent with the small particle sizes inferred from the SME data of mean radius of 43±16 nm, with all cases smaller than 100 nm [Rusch *et al*., 1991]. Very early results from a new study of the presence of PMCs in the SAGE II data, show a number of PMCs in both hemispheres in every PMC season since SAGE II began operation in 1984, (Shettle, Thomason, and Burton, 1999; unpublished results). The frequency of occurrence and brightness of the PMCs is a strong function of both season and latitude. They primarily occur during a 13-week period centered about 2 weeks after the summer solstice in each hemisphere. From the SME observations they cover most of the summer polar region, poleward of 70 to 75 degrees [Thomas and Olivero, 1989]. They decrease in both frequency & brightness going towards lower latitudes, becoming virtually non-existent equatorward of 50 degrees. This means the METEOR SAGE III, probably will not see any PMCs, or possibly a only handful in the Northern summers, since the METEOR SAGE measurements are furthest from the pole Near the summer solstice. However the measurements from the Space Station SAGE III will get to high enough latitudes during the PMC season, to see a number of PMCs.

Given even a relatively thin PMC could contribute a non-negligible signal in the 290 nm channel which will be used by SAGE III to measure high altitude ozone, it will be important to screen even the METEOR SAGE III measurements for possible evidence of PMCs to avoid their interfering with the ozone retrievals.

2.4   Cloud Presence Experimental Objectives

The experimental objective is to identify the presence of cloud along the optical path from the sun to the SAGE III instrument. As discussed in Section 2.2, cloud causes an increase in the extinction at all measurement wavelengths. In particular, for the purposes of determination of cloud presence, an increase occurs in the aerosol channels. With certain assumptions, and by making use of data obtained at more than one wavelength, the presence of cloud may be deduced. As originally proposed, the sole cloud product for each measurement event was to be the maximum altitude at which cloud was found for that event. This objective is now considered too narrow and the objective of the algorithm in this ATBD is to identify the presence or absence of cloud over a range of altitudes. This altitude range will extend from the lowest altitude at which sufficient aerosol extinction data is available to resolve cloud, upward, to 30 km. The chosen method for resolving cloud depends upon the existence of inverted data in the 521, 1020, and 1540 nm aerosol channels. Due to attenuation by aerosols and the molecular atmosphere, the signal amplitude in the 521 nm channel is likely to fall below a useable level at an altitude of about 6 km. Thus, the present algorithm will not be able to identify the presence of cloud below this altitude. If cloud at a higher altitude cause total extinction of the signal for a given event, then that altitude becomes the lower limit. The search for cloud will be carried out up to an altitude of 30 km in order to include polar stratospheric clouds in the database.

3.0 Algorithm Description

This section describes in detail the SAGE III cloud presence detection algorithm, including methodologies for identifying opaque and non-opaque clouds, input and output data, the structure of the algorithm itself, and data validation considerations.

3.1 SAGE III Measurement Approach

SAGE III will be making aerosol measurements at wavelengths of 385, 448, 521, 670, 758, 869, 1020, and 1540 nm. The Solar and Lunar ATBD describes how the SAGE III transmission data at these wavelengths are inverted to give a set of vertical extinction profiles. These profiles, which have a vertical resolution of 0.5 km (in contrast to the 1.0 km vertical resolution for SAGE III predecessors), have been corrected for non-particulate extinction and thus show the combined extinction due to aerosol and cloud only. The problem discussed in this section is that of separating the effects due to cloud from that due to aerosol using data from one or more wavelengths. The shortest wavelengths do not provide useful data at tropospheric altitudes, where most cloud occurs and we consider data only for wavelengths 521 nm through to 1540 nm.

The measurement geometry of the SAGE III instrument is shown in Figure 3.1.1 and is the same as that employed by its predecessors. During each spacecraft sunrise and sunset, SAGE III will measure the horizontally attenuated solar radiation. Two measurement events thus occur for each spacecraft revolution. These are inverted to give vertical profiles of aerosol extinction and gaseous concentrations down to altitudes where the signal received at the satellite instrument falls below the threshold level of the instrument. SAGE III will make 14-15 sunrise and a similar number of sunset measurements per day, each separated by approximately 24° in longitude and a much smaller change in latitude. The latitude coverage depends upon spacecraft orbital inclination and right ascension. Typical coverage for solar measurements only is shown in Figure 3.1.2 for launch onboard the Meteor spacecraft (1020 km altitude, sun synchronous orbit) and on Space Station (375 km altitude, 51.6° inclination orbit). The former orbit provides coverage in medium to high latitudes only with some seasonal variation. The latter provides coverage of low and medium latitudes but not the polar regions, and repeat coverage of a latitude occurs about every three weeks. The description of the instrument characteristics given in Appendix A includes mention of the use of SAGE III for lunar as well as solar occultation measurements. Because of the reduced signal/noise, such measurements will be limited to altitudes above 15 km eliminating almost all of the troposphere. As a consequence, lunar data is not at present being considered for cloud retrieval.

The operation of the SAGE III instrument during each occultation measurement will be totally automatic. Prior to each occultation event, the instrument will rotate in azimuth to its predicted solar acquisition position. When the sun enters the instrument's field of view, the instrument will lock onto the radiometric center of the sun in azimuth. The elevation

scan mirror will then perform vertical scanning across the solar disk with a scan rate of 15 arcminutes per second. Radiometric data will then be sampled at 64 samples per second per channel for the solar measurements, and digitized to 14-bit resolution. Radiometric data will be taken when the sun is between sea level or cloud top up to 300 km altitude at the tangent point.

The raw-count data from the SAGE III telemetry will be converted into atmospheric transmission versus tangent altitude data for each channel by first processing the combined information from the spacecraft, solar, and earth ephemeris data together with atmospheric refraction correction to provide proper measurement location determination. Radiometric calibration will then be performed by normalizing the solar scan data obtained within the atmosphere with the high-altitude solar limb profile obtained at each radiometric channel. The transmission profile data will then be converted into profiles of limb optical thickness as a function of tangent height in the atmosphere for each radiometric channel centered at each wavelength. These data will then be inverted into vertical profiles of aerosol and other gaseous species as described in the Solar and Lunar ATBD. A detailed description of the procedure for the generation of the limb transmission profiles at each wavelength channel is also included in the SAGE III ATBD on transmission data products.

Since the occultation technique utilizes the long optical path geometry in a spherical atmosphere to provide for the high sensitivity in measurement capability, the presence of cloud in the field of view will normally produce a very strong signature. For a thin cloud with large horizontal extent, the SAGE III instrument should be able to obtain good extinction measurements of the cloud property provided the average extinction is not so high as to nullify the transmitted signal, and the field of view of the instrument is less than the vertical extent of the cloud thickness, (in this case about 0.5 km). For horizontally extended thin cloud with thickness smaller than the vertical field of view of the instrument, the measured transmission data will reflect a spatially averaged cloud extinction property. In most cases for thick clouds, the sun scan measurements will be blocked somewhere near the cloud top, depending on the extinction property of the cloud. The transmission profiles for all channels in this case will be terminated at the height where the transmitted signal is close to a threshold value still to be defined (~0.1 % of exoatmospheric signal) at the 1540 nm wavelength. If the transmission profile reaches this threshold value at a certain height, any transmission measurements obtained below this height will not be used for aerosol profile retrieval. For cases where the horizontal extent of the cloud is small, the situation can become very complicated, and will not be discussed here.

Figure 3.1.3 shows typical inverted aerosol extinction profiles at wavelengths of 525 nm and 1020 nm that were obtained with the SAGE II instrument. The three panels of this figure show respectively (a) a cloud-free aerosol profile extending down to the lower troposphere, (b) a profile on which thin cloud is present at high altitude and (c) a profile that terminates near the tropopause because of the presence of thick cloud. Error bars are shown on all six curves. In figure panel 3.1.3(a) inversion of data at 525 nm is terminated at 6.5 km because of the low signal, while that for 1020 nm in the same panel goes to a

lower altitude. Non-opaque cloud is shown in panel 3.1.3(b), where the profiles continue below the cloud. Note: the anomalously low value of the 525 nm extinction just below the cloud, the large associated error bar and that the ratio of the extinctions at the two wavelengths becomes approximately unity within the cloud layer. A third possibility is shown in panel 3.1.3(c) where the extinction profiles at both wavelengths terminate at the cloud altitude. As discussed in Section 2.3, much of the cloud detected by SAGE II is subvisual, that shown in panel 3.1.3(b) probably falls within this category. The cloud causing the cut-off shown in panel 3.1.3(c) would most likely just be visible. The profiles shown in Figure 3.1.3 are not exhaustive; for example it is possible for cut-off due to cloud or aerosol to occur at the 525 nm wavelength and not at 1020 nm (under these conditions the presence of cloud becomes indeterminate). It is anticipated that profiles similar to those shown for SAGE II in Figure 3.1.3 will be obtained with SAGE III, but they will have superior vertical resolution (0.5 km versus 1.0 km) and will be available at a larger number of wavelengths.
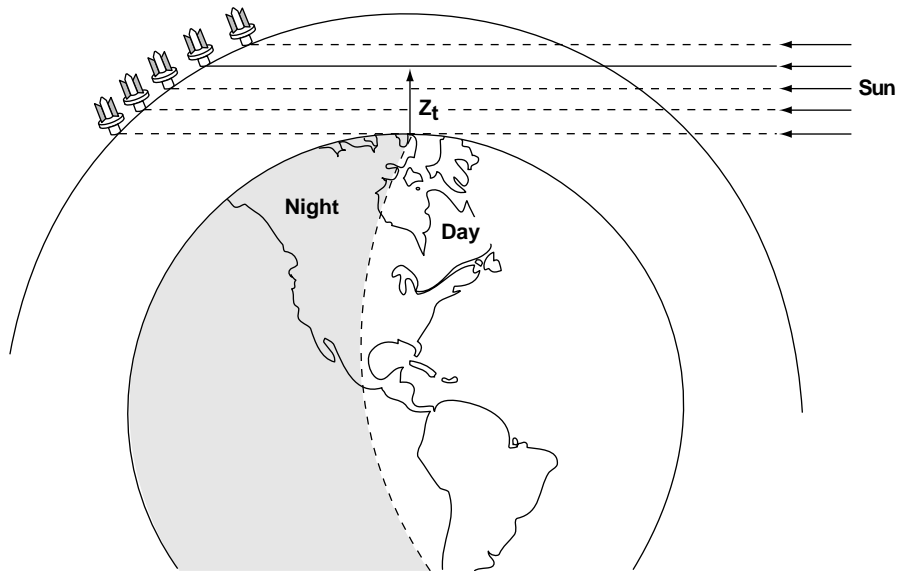
Figure 3.1.1 SAGE III solar occultation measurement geometry. The tangent altitude is denoted by Z_t.
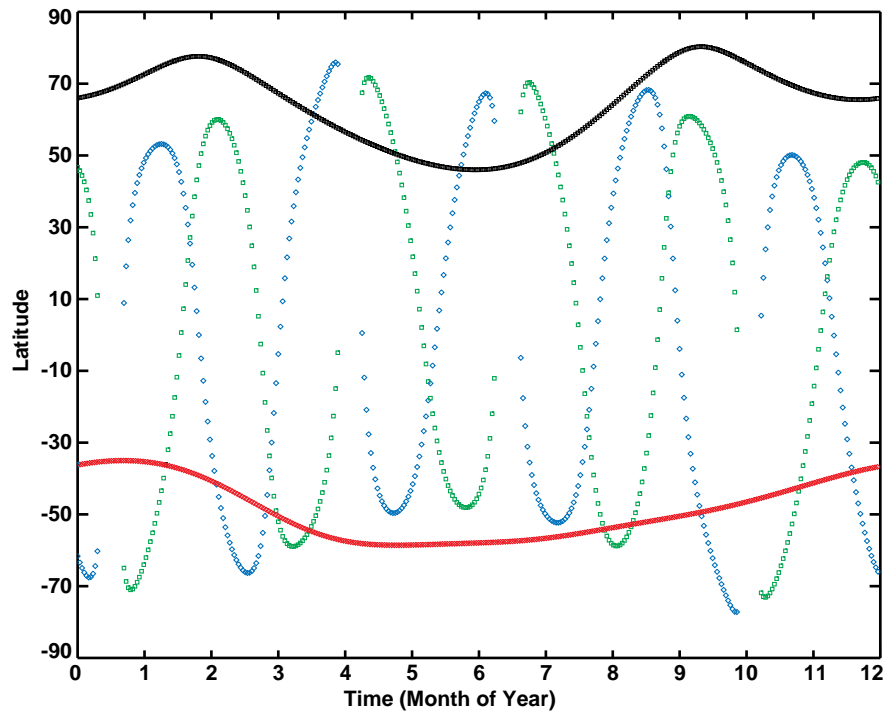
Figure 3.1.2 Time-latitude coverage of SAGE II measurement opportunities for 1998 and 1999. Sunrise events are indicated by green symbols and sunset events by blue symbols. The time-latitude coverage for Meteor/SAGE III is overlaid to show near-coincident measurement opportunities between satellite instruments.
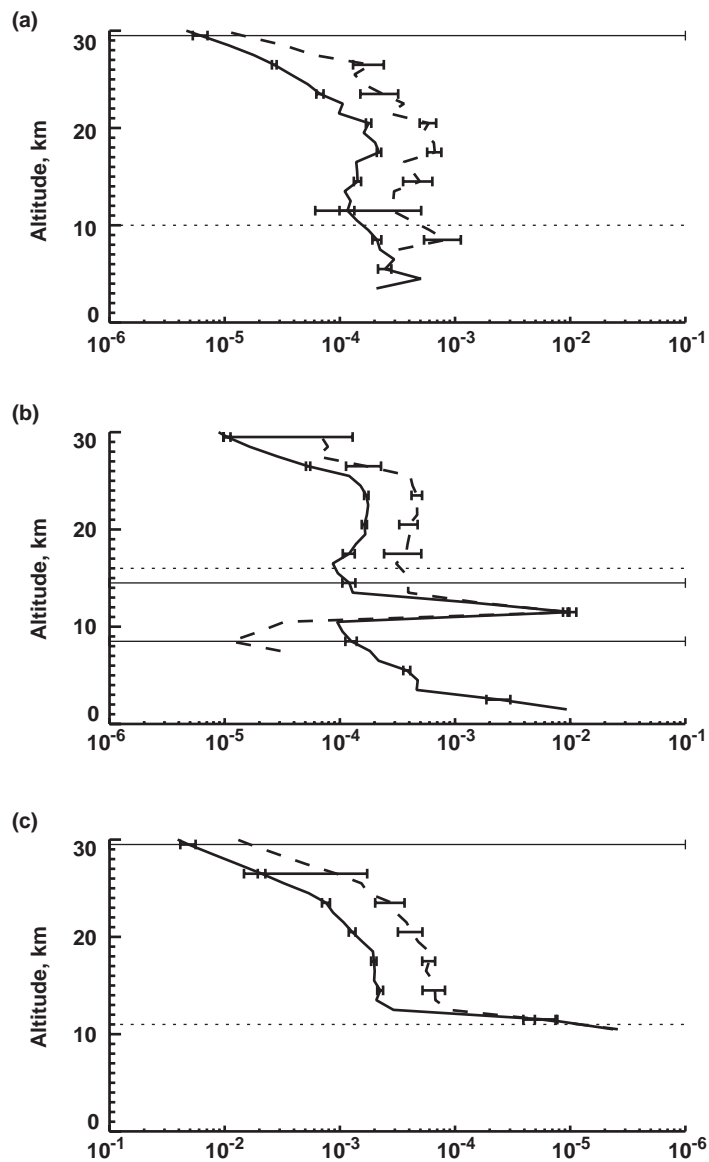
Figure 3.1.3   Typical inverted aerosol extinction profiles at wavelengths of 525 nm (dashed lines) and 1020 nm (solid lines) that were obtained with the SAGE II instrument. The three panels of this figure show respectively (a) a cloud-free aerosol profile extending down to the lower troposphere, (b) a profile on which thin cloud is present at high altitude and (c) a profile that terminates near the tropopause because of the presence of thick cloud. Error bars are shown on all six curves.

3.2   Methods for Cloud Presence Identification

3.2.1   Opaque Clouds

The algorithm described in the next section assumes that radiation is received at the satellite from the sun at all three wavelengths. As we have seen in Figure 3.1.3, this is not always the case. Inversion of extinction data at 525 nm is stopped at an altitude of 6.5 km because of the low signal levels below that altitude. Most profiles at 1020 nm do not reach to the Earth's surface due to excessive attenuation of the signal, and similar behaviour is to be expected for the 1550 nm channel on SAGE III. Such termination occurring in the upper troposphere or in the polar stratosphere is believed to be due to the presence of opaque cloud along the optical path from the sun to the satellite instrument. The equivalent vertical optical depth of the cloud for which termination just occurs depends upon the cloud geometry, but is of the order of 0.05, i.e. the cloud is very thin but not subvisual. At times of high volcanic aerosol content, such as that following the Pinatubo volcanic eruption, the extinction produced by the volcanic aerosol may also be large enough to cause profile termination [McCormick and Veiga, 1992], sometimes at very considerable altitudes. At non-volcanic times these occurrences are believed to be due only to cloud. They will be noted and the data flagged accordingly; the altitude assigned to the cloud will be 0.5 km below that of the last data point on the profile. At altitudes within a few km of the tropopause the number of terminating profiles is found to be considerably less than the number of profiles showing non-opaque cloud. As we proceed to lower altitudes, the number of terminating profiles increases markedly. Occasionally a profile may terminate at one or two wavelength only, even for altitudes above 6.5 km. In such cases it is not possible to determine if cloud is present or not.

3.2.2   Non-opaque Cloud - Basic Method

Clouds of lower optical density than those causing full signal loss will attenuate the signal, yielding measurable extinction values that vary with wavelength. This wavelength variation will differ, depending on whether cloud or aerosol produces the attenuation. Aerosol/cloud separation methods used with SAGE II data, described in Section 2.3, are based on the differential variation of extinction with wavelength and use the values of the extinction obtained at wavelengths 525 nm and 1020 nm. Two methods in particular were discussed, the more widely used slope/intercept method and the slope method. SAGE III offers a wider choice of wavelengths; data at 1540 nm are likely to be particularly useful, as they offer the opportunity for better discrimination for cloud particulate scattering in the presence of large volcanic aerosols. The proposed algorithm for use with SAGE III data uses the extinction data at wavelengths 521 nm, 1020 nm and 1540 nm. Simulation studies [Kent *et al.*, 1997b] have been carried out in order to determine how such an algorithm might be expected to perform. For comparison purposes, similar simulations have been carried out using both methods noted above with the SAGE II wavelengths and with the two longest SAGE III wavelengths only these simulations were carried out

at the proposed SAGE III wavelengths of 525, 1020, and 1550 nm rather than at the actual wavelengths of 521,1020, and 1540 nm. Extinction data obtained at 670, 758, and 869 nm have not been included in these simulations. These may form the subject of future work, although it is unlikely that these data will greatly improve the algorithm performance, except in so much as the errors at these other wavelengths may be less than those at 521 nm.

Simulations Using In-Situ Data

As input to these simulations, over 100 in-situ measured aerosol size distributions have been obtained from published literature [Knollenberg and Huffman, 1983; Oberbeck *et al*., 1983; Snetsinger *et al*., 1992; Deshler *et al*., 1993; Pueschel *et al*., 1993; Wilson *et al.,* 1993; Goodman *et al*., 1994; Pueschel *et al.,* 1994] and used to derive wavelength dependent values for the aerosol extinction. These measurements cover the time period 1981 - 1993, and altitudes from the upper troposphere to the stratospheric layer maximum. Most data is recent post-volcanic, as the majority of research flights have been made at these times. For the purposes of statistical intercomparison, data have been divided into the following two classes: (1) Data taken within 2 years after the eruption of either El Chichon (April, 1982) or Pinatubo (June, 1991) [94 measurements], and (2) Background (excluding the above time periods) [11 measurements]. Cloud has been simulated using SAGE II upper tropospheric data. Specifically, the simulated cloud, whose extinction distribution has been added to that of the aerosol, is the annual mean for that (by amount and extinction) found at low latitudes at an altitude of 16.5 km.

Theoretical Basis for Earlier Aerosol / Cloud Discrimination Methods

The theoretical basis for the slope, [Wang *et al*. 1994], and slope and intercept, [Kent *et al.* 1993], methods used with SAGE II data are shown in Figure 3.2.1. Both figure panels show the expected relationship between the extinctions at 525 nm and 1020 nm. The solid black areas show the location of aerosol extinction data points where, for background aerosols, the extinctions are small and the ratios of the extinctions lie between about 3 and 5. Cloud extinction values are larger and the ratio is approximately unity. In both figures dashed lines have been drawn to separate the aerosol and cloud. For the slope and intercept method (figure panel 3.2.1(b)), the appropriate line constants are determined from the statistical behaviour of the aerosol subset. For the slope method, the slope may also be determined from the data subset itself or a constant value chosen. Wang *et al.,* [1994] studied one year of tropical aerosol and cloud data and used a constant slope of 2.1. The advantage of using a constant value lies in the fact that a data accumulation (typically for three months) is not required. Against this must be set the fact that determining the slope, or slope and intercept, from appropriate subsets of a global data ensemble may be expected to provide better values for these constants. In the analysis presented below we have determined the parameters for the slope and intercept method from the actual data sets used, for the slope method we have used a constant slope value of 2.0. The SAGE III methods considered use both constant and data derived parameters.

Proposed Method for use with SAGE III Data

The theoretical basis for the method that is proposed for use with the SAGE III data is shown in Figure 3.2.2. Figure panel 3.2.2(a) shows a plot of the (525 nm/1020 nm) extinction ratio versus the (1020 nm / 1550 nm) extinction ratio calculated for monodisperse aerosol size distributions. The composition is assumed to be 75% sulphuric acid, and data points are computed at equal logarithmic radius intervals of 1.122 (10.05). Numbers adjacent to the curves give the particle radii in micrometers; Figures 3.2.2(a) and 3.2.2(b) are identical except for a scale change. Cloud is shown by a dot at location (1.0, 1.0). Increasing amounts of cloud cause the data points to move away from the aerosol curve and towards the (1.0, 1.0) point, as shown by the arrows in the top panel. The shaded area in panel 3.2.2(b) has been chosen to delineate the region of the plot where the data may be supposed to show the presence of significance amounts of cloud. Data points outside this area will be taken to be aerosol. The shape and size of this area was determined on the basis of the simulation studies. As will be shown below, under background aerosol conditions, no major problems are found in the separation of the two constituents. Under volcanic conditions, exact separation is not possible. The area shown here is one for which the errors arising from two separate error conditions are approximately equal in number. In the first error condition, the cloud set will contain additional non-cloud data points due to the presence of large aerosols, which have extinction values that are insensitive to wavelength. In the second error condition, cloud data points representing very thin cloud occur outside this area, they are classified as aerosols and so are lost from the total cloud count.

Figure 3.2.3 and Figure 3.2.4 show scatter plots of the (525 nm / 1020 nm) extinction ratio versus the (1020 nm / 1550 nm) extinction ratio for the background and volcanic situations. These have been calculated from in-situ measured size distributions described earlier. The aerosol data points are shown by solid dots, those with added cloud by crosses. It can be seen that, although these calculations are for real aerosol size distributions, the distribution of the majority of the aerosol extinction ratios is very similar to that shown for monodisperse size distributions in Figure 3.2.2. There is nevertheless some scatter in the data values in Figures 3.2.3 and 3.2.4 due to the continuous nature of the measured aerosol size distributions and the possible occurrence of more than one mode within a single size distribution (one background data point in particular has a quite anomalous value). The distribution of cloud extinction values that has been added, was calculated from the annual mean behaviour observed by the SAGE II instrument in 1988, between 20°S and 20°N, at an altitude of 16.5 km. This distribution, which in practice is continuous, has been discretised in units of 1.0×10^{-6} m^{-1}. This unit is a few times greater than the extinction of background aerosol at a wavelength of 1020 nm but considerably less than that due to the El Chichon or Pinatubo volcanic aerosols. Use of other cloud distributions will undoubtedly lead to different figures for algorithm performance but will not necessarily change significantly the relative performance of different methods for separating aerosol and cloud. As was done in Figure 3.2.2, the same data are shown with different scales in each of the panels of Figures 3.2.3 and 3.2.4. Figure panels 3.2.3(b) and 3.2.4(b) show the area chosen for selection of cloud data as was shown in Figure 3.2.2(b). In the case of the non-volcanic

aerosol size distributions shown in Figure 3.2.3 there is complete separation of cloud and aerosol. For the volcanic aerosol shown in Figure 3.2.4, separation is incomplete and it is clear from the overlap between aerosol, and aerosol plus cloud, data points that no perfect separation is achievable. Small movements of the boundaries of the shaded area change the error rate within the two error classes discussed above but make little change to the total error rate.
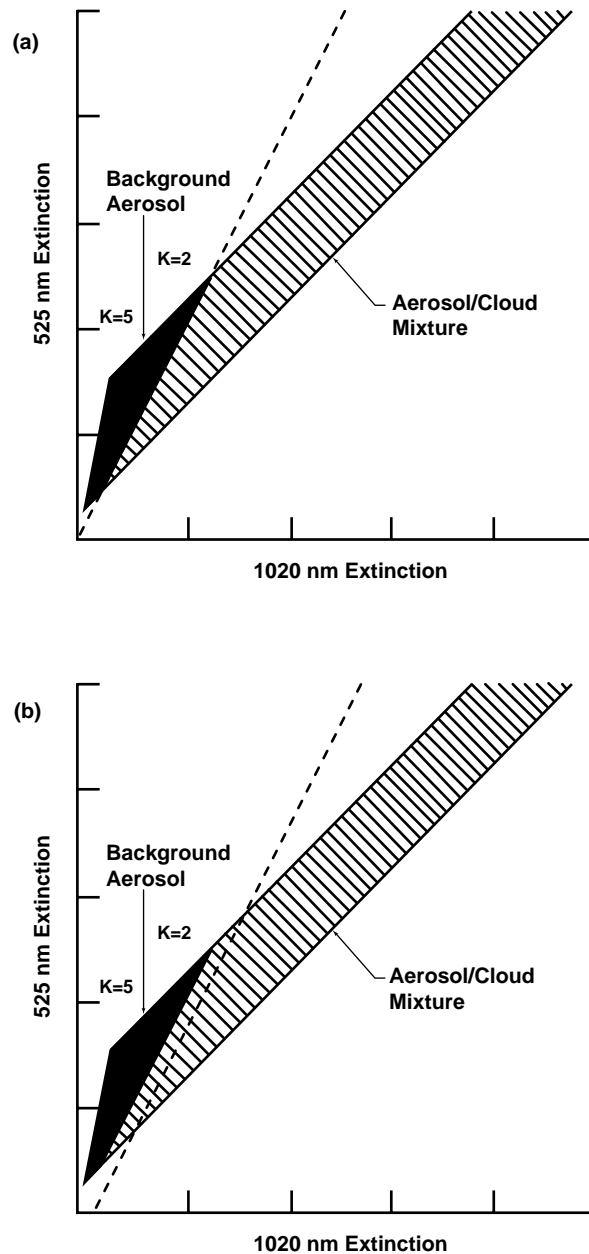
Figure 3.2.1 Theoretical basis for (a) the slope method and (b) the slope and intercept method of separating aerosol and cloud in the SAGE II data set.

28
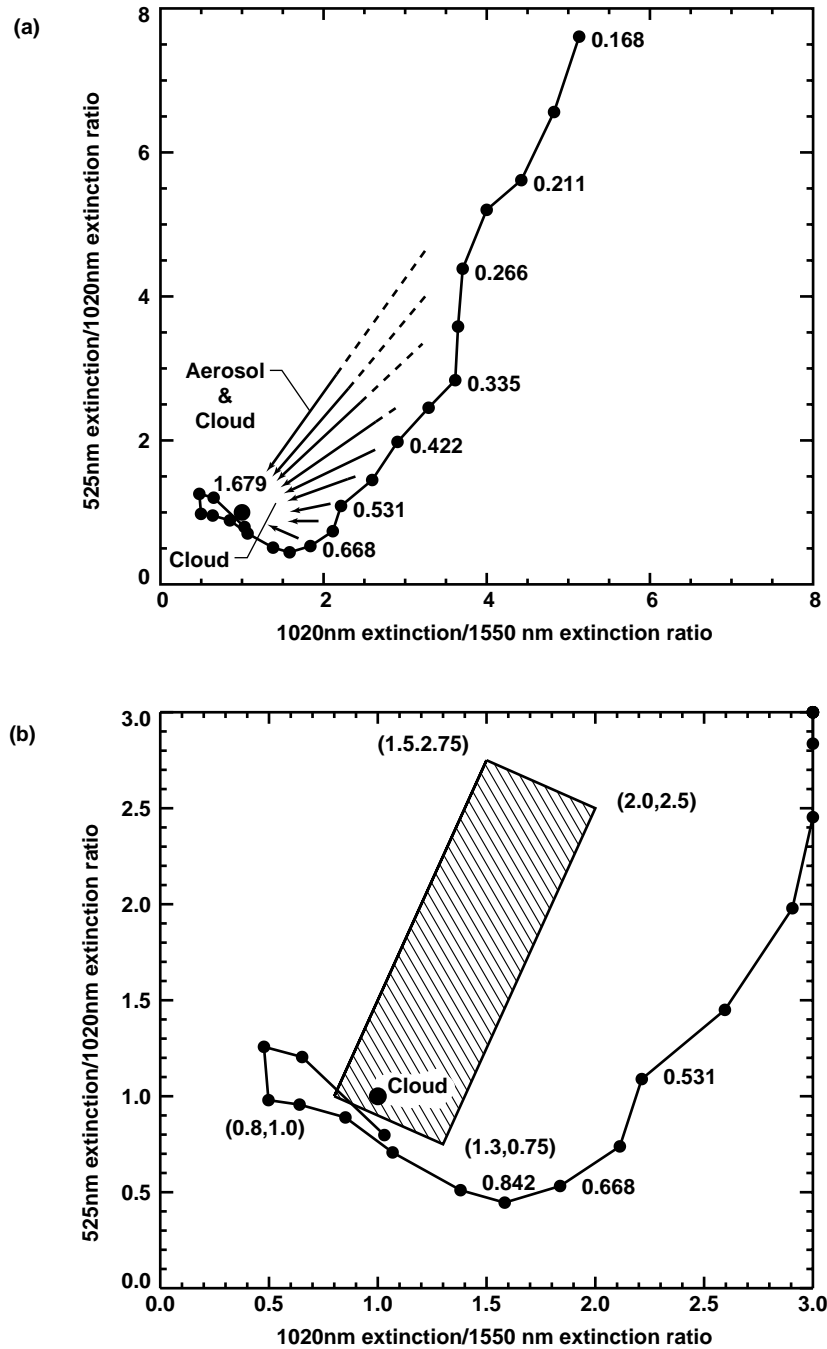
Figure 3.2.2 Theoretical basis for the proposed method of separating aerosol and cloud in the SAGE III data set. The continuous curves show the relationship between the 525 nm / 1020 nm and the 1020 nm / 1550 nm extinction ratios for monodisperse size distributions. Solid dots show the individual data points. Calculations have been made for a 75% sulphuric acid composition. Numbers adjacent to the curves show the particle radii in micrometers. Cloud is shown by the large dot at location (1.0,1.0). Panels (a) and (b) show the same data plotted to different scales, data points within the shaded area in panel (b) are considered to correspond to cloud as well as aerosol along the optical path.

29
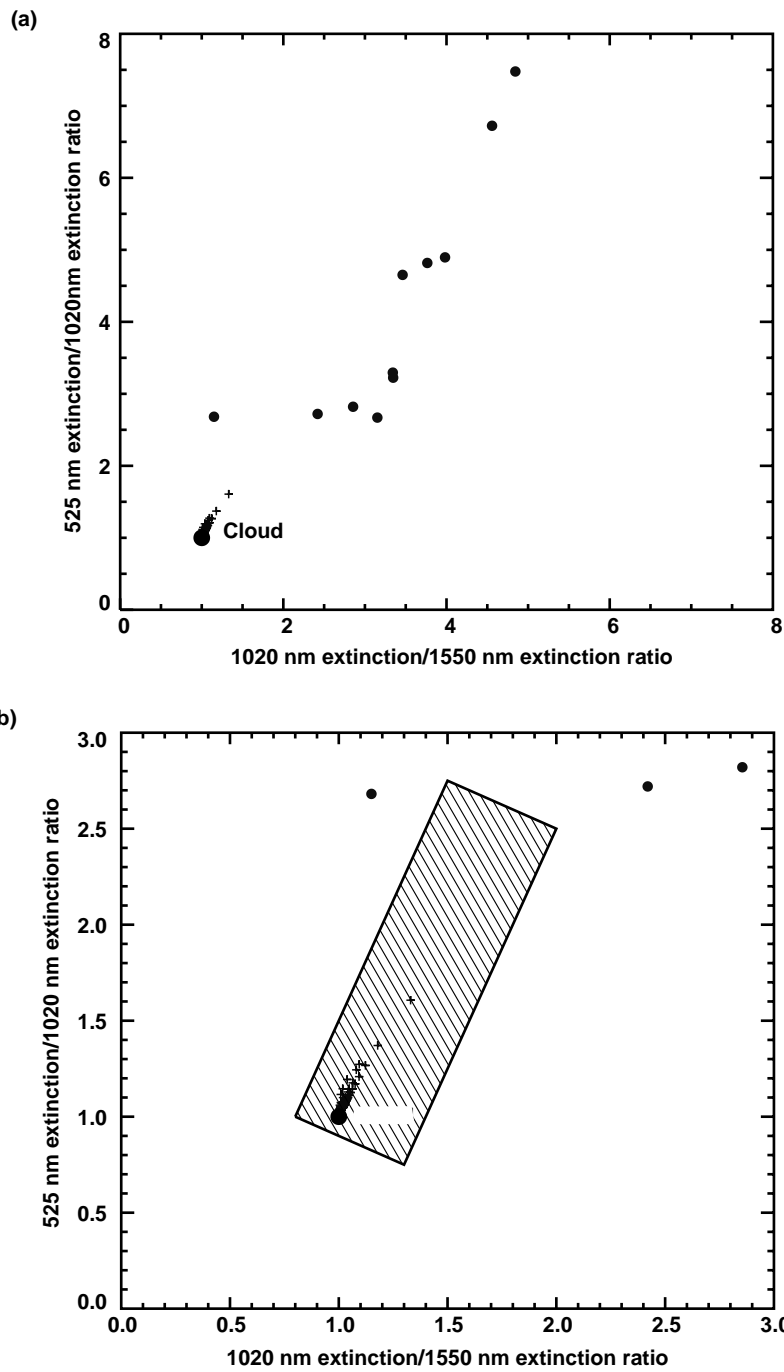
Figure 3.2.3 Scatter plots of the 525 nm / 1020 nm and the 1020 nm / 1550 nm extinction ratios for in-situ measured size distributions during non-volcanic conditions. Solid points correspond to aerosol data only, crosses correspond to aerosol plus different amounts of simulated cloud. Plot scales and the shaded area, which is used in the algorithm to determine the presence of cloud, are the same as in Figure 3.2.2.
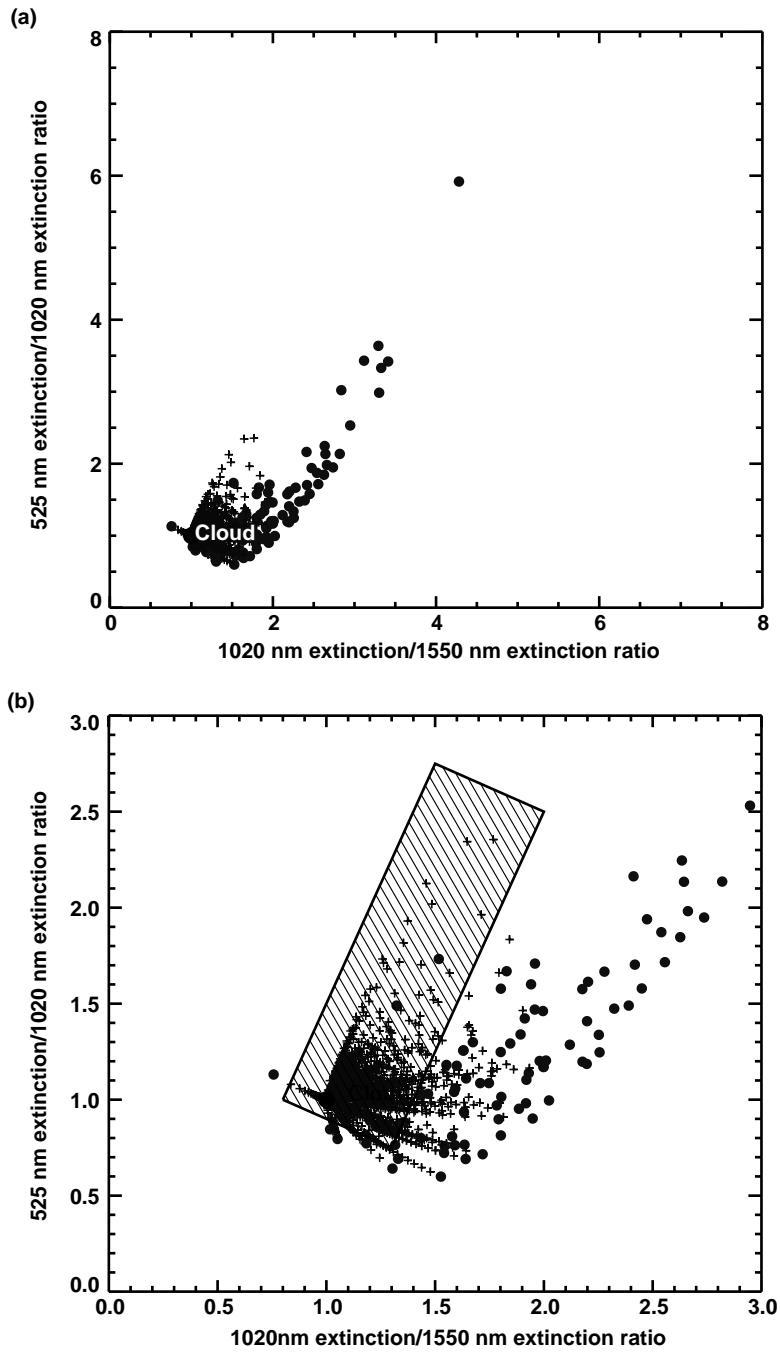
Figure 3.2.4 As for Figure 3.2.3, but with volcanic aerosol present.

Performance Intercomparisons

Performance intercomparisons have been made between the method for aerosol-cloud separation just described (denoted as method 1) and four other methods. Method 2 is the slope method using data at 525 and 1020 nm, with a value of 2.0 chosen for the (525 nm / 1020 nm) extinction ratio used to separate aerosol and cloud. Method 3 is the slope and intercept method using data at 525 nm and 1020 nm, with optimum values for the slope and intercept determined from the data subsets. Method 4 is the slope method using data at 1020 and 1550 nm, with a value of 1.5 chosen for the (1020 nm / 1550 nm) extinction ratio used to separate aerosol and cloud. Method 5 is the slope and intercept method using data at 1020 nm / 1550 nm, with optimum values for the slope and intercept determined from the data subsets.

Methods 2 and 3 are the same as those described earlier as having been used with SAGE II data. Methods 4 and 5 are essentially the same as methods 2 and 3, but employing the extinctions measured at the two longest SAGE III wavelengths only. Errors in the measured cloud occurrence can occur as a loss of true cloud points (*cl*) from the identified cloud subset and the inclusion into that region of unwanted contaminating aerosol points (*ag*) To provide a quantitative measure of the success of a method an error rate (*er*) has been defined as

$$er = (cl^2 + ag^2)^{0.5}$$

where *er, cl*, and *ag* are expressed as fractions or percentages of the true cloud amount in the subset. Table 3.2.1 below shows the result of this analysis for both volcanic and non-volcanic conditions. The values shown for the error rate of each method are the lowest that could be found for any values of the variable parameters (methods 3 and 5).

Table 3.2.1 Cloud presence error rate as a function of method and aerosol condition.

Method	Aerosol Condition	Cloud Loss Rate (%)	Contamination Rate (%)	Overall Error Rate (%)
1. Three wavelength method	Background Volcanic	0.0 21.7	0.0 19.1	0.0 28.9
2. Slope method (525 and 1020 nm)	Background Volcanic	0.0 1.0	0.0 220.0	0.0 221.0
3. Slope and intercept method (525 and 1020 nm)	Background Volcanic	0.0 56.4	0.0 32.7	0.0 65.2
4. Slope method (1020 and 1550 nm)	Background Volcanic	0.0 14.6	23.3 49.1	23.3 51.2
5. Slope and intercept method (1020 and 1550 nm)	Background Volcanic	0.0 34.2	0.0 21.8	0.0 40.6

The table shows that methods 1, 2, 3, and 5 all work well with background aerosols. Method 2 shows very large errors when volcanic aerosols are present, which is to be expected since the constant slope value of 2.0 is applicable to background aerosols (from 1989) and not suitable for volcanic conditions. A better slope value could be found, but the performance of the method is not likely to be better than that of the analogous slope and intercept method (3). Methods 3, 4, and 5 all show error rates in the range 40% to 60% under volcanic aerosol conditions. Of these three methods, the best is the slope and intercept method using the longer two wavelengths of SAGE III. The best overall results are obtained with method 1 using wavelengths 525, 1020 and 1550 nm.

The error rates achievable with method 1 during volcanic conditions, even though lower than those shown for the other methods, may still be unacceptably high for many research purposes. Such conditions do not last for a great length of time. This is illustrated in Figure 3.2.5, which shows the cloud presence error rate as a function of time between 1982 and 1993. Each point in these plots represents one in-situ measurement. Errors of both kinds (cloud loss and cloud contamination) commence about 6 months after the eruptions of El Chichon and Mt. Pinatubo. As seen in the post-Pinatubo data, recovery begins about one year after the eruption. In the case of El Chichon, data taken two years and longer after the eruption showed no ambiguities.
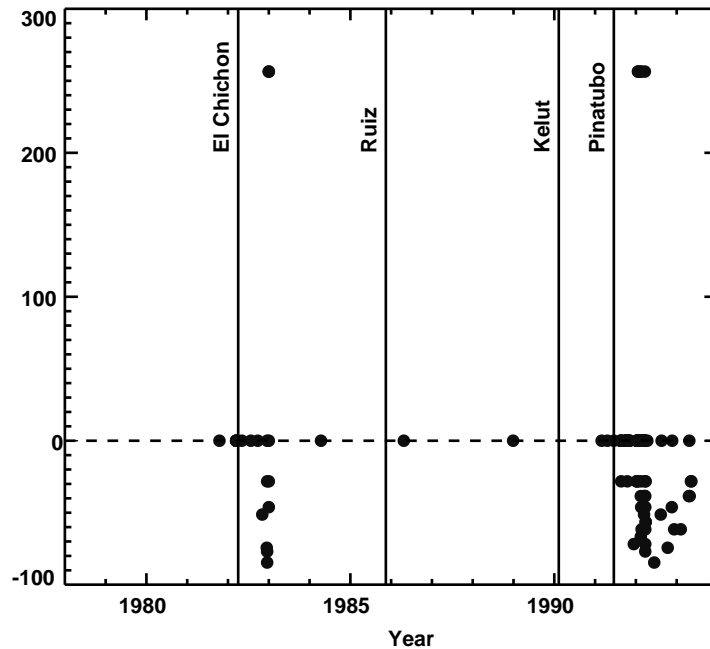
Figure 3.2.5 Cloud presence error rate, % as a function of time of measurement. Positive errors indicate contamination of cloud by aerosol, negative errors indicate loss of cloud data prints. Each data point represents one in-situ measurement, most of which were made at times of volcanic activity. The concentration of errors during the periods following the eruptions of El Chichon and Mt. Pinatubo is obvious.

3.2.3   Non-Opaque Cloud - Refinements

Following a volcanic eruption it is not possible to obtain an unambiguous separation of aerosol and cloud. Even using the three wavelength method, there are cloud loss and contamination rates of about 20%. These rates may be altered by shifting the boundaries of the area used to identify the presence of cloud. This is illustrated in Figure 3.2.6, which shows the effects of shifting the location of that edge of the identifying parallelogram where the majority of the ambiguity occurs. The dashed lines in Figure 3.2.6(a) indicate the different positions of this edge for which calculations have been carried out, the positions of the edge being specified by the coordinates of its upper and lower ends. The results of this operation as they effect the loss and contamination rates are shown in Figure 3.2.6(b) and Table 3.2.2.; the figure and table also show the effects on aerosol identification. The results may be summarised qualitatively as follows:

- As the selection area is decreased (larger ycc) the rate of corruption of cloud by volcanic aerosol decreases, while the loss rate of cloud increases

- As the selection area increases (smaller ycc) the rate of corruption of aerosol by cloud decreases, while the aerosol loss rate increases.

34

- Shifting the boundary can clearly be used to reduce the effect of corruption of either aerosol or cloud by the other. An unfortunate aspect of these results is that in both cases, as we achieve a greater certainty of the component that we are identifying, the loss rate of that component is found to increase even faster. Thus, reducing the cloud corruption rate from 20% with a concurrent loss rate of 20%, to a cloud corruption rate of 10% raises the loss rate to about 50%.

- The algorithm performance for aerosols shown in Table 3.2.2 is better than that for cloud. The relative performance is dependent upon the amount of cloud present, and under high cloud conditions could be biased in the opposite direction.

- The calculations just described are for the atmospheric conditions encountered within two years after the eruptions of either El Chichon or Pinatubo. Examination of the effect of changing the area boundaries as just described, for background aerosol conditions, shows no change in algorithm performance.

In order to supply additional information to the data user, cloud presence will be supplied in the form of an index whose value depends upon the location of the data point in relation to the cloud detection areas shown in Figure 3.2.6(a). These are redrawn in simplified form in Figure 3.2.7, which also shows the corresponding values of the data indices (from 1 to 4). The coordinates of the right-hand side of the parallelogram are reproduced in Table 3.2.3, together with the relevant index values. Further details on the algorithm will be given in Sections 3.5 and 3.6.

Table 3.2.2 Results of modifying cloud selection area in

Aerosol / cloud separation algorithm (volcanic conditions only)

xcc	ycc	Aerosol Corruption Rate (%)	Aerosol Loss Rate (%)	Cloud Corruption Rate (%)	Cloud Loss Rate (%)
1.10	.850	18.6	4.3	10.9	47.6
1.15	.825	15.6	5.3	13.6	40.0
1.20	.800	12.8	6.4	16.4	32.8
1.25	.775	10.0	6.4	16.4	25.6
1.30	**.750**	**8.5**	**7.4**	**19.1**	**21.7**
1.35	.725	7.1	12.8	32.7	18.3
1.40	.700	6.0	14.9	38.2	15.5
1.45	.625	4.4	22.3	57.3	11.4
1.50	.650	3.8	24.5	62.7	9.7

(a)

(b)
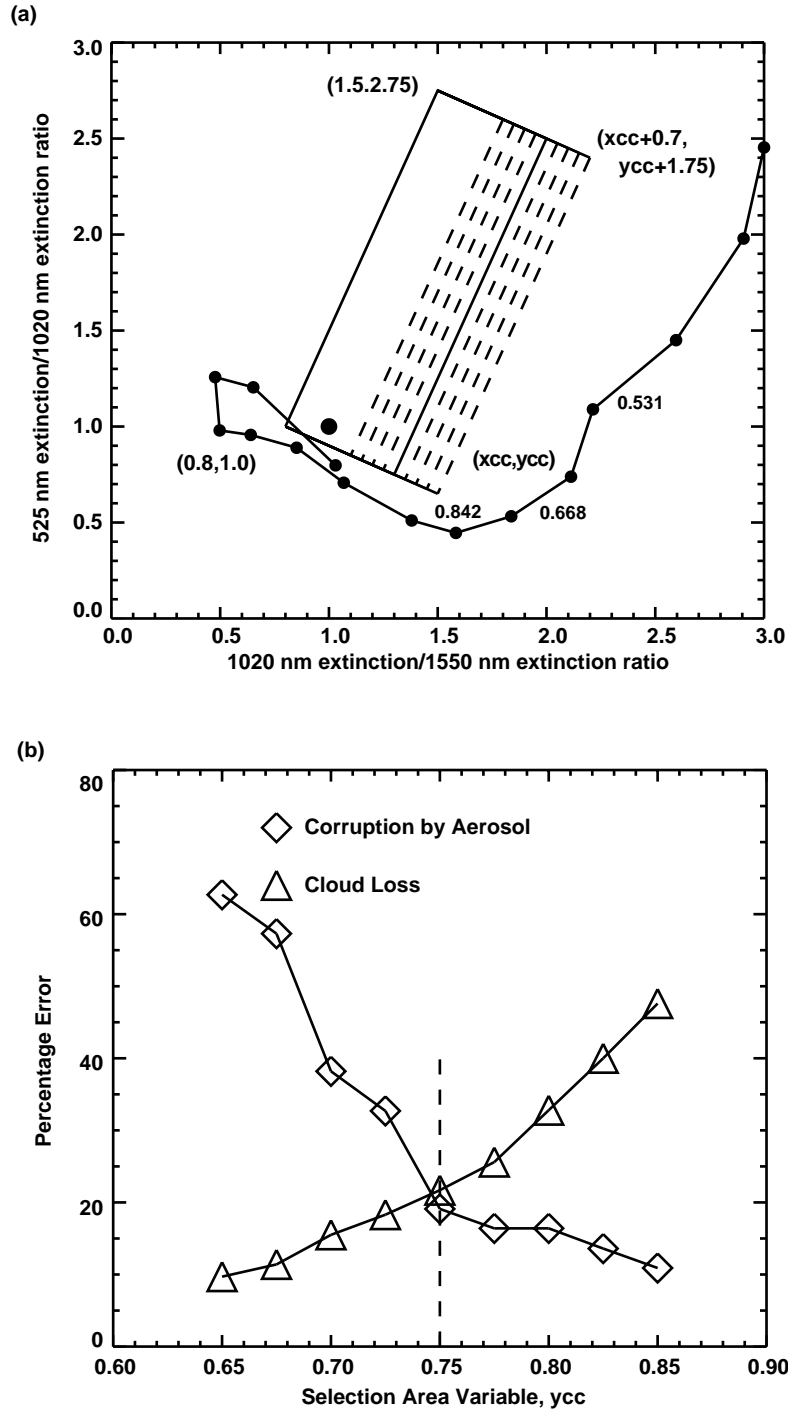
Figure 3.2.6 (a) Alternative cloud selection areas for which simulations have been carried out. The coordinates of the ends of the dashed lines are given in Table 3.2.2. (b) Effect of changing the cloud selection area, as shown in (a), on cloud loss and corruption rates under volcanic conditions.

Table 3.2.3 Recommended parameters for the end points

of the right hand edge of the cloud area parallelogram.

Relevant Data Indices	xcc	ycc	Aerosol Corruption Rate (%)	Aerosol Loss Rate (%)	Cloud Corruption Rate (%)	Cloud Loss Rate (%)
4, 3	1.10	.850	18.6	4.3	10.9	47.6
3, 2	**1.30**	**.750**	**8.5**	**7.4**	**19.1**	**21.7**
2, 1	1.50	.650	3.8	24.5	62.7	9.7
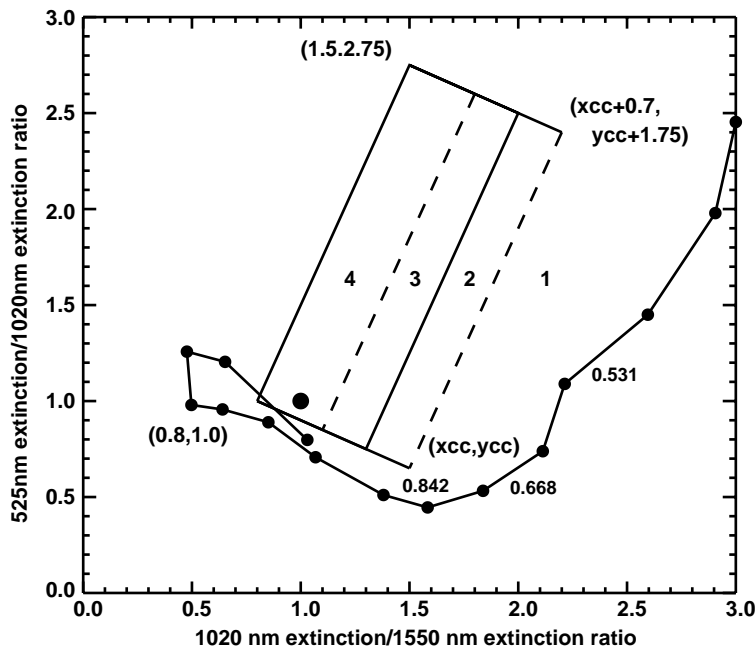
Figure 3.2.7 Figure showing the areas chosen for use in the cloud presence algorithm. Each area is designated by a index value between 1 and 4; end point coordinates for the right hand movable edge of the cloud parallelogram are given in Table 3.2.3.

3.3   Inhomogeneity Problem

A basic assumption in the inversion scheme used to obtain the vertical profile of aerosol extinction is that the atmospheric constituents are horizontally homogeneous. While this is an acceptable assumption for stratospheric aerosol, and possibly for tropospheric aerosol as well, it is clearly not true for cloud. In their statistical intercomparison of the SAGE II and ISCCP cloud data sets, Liao *et al*, [1995a] deduced a mean horizontal cloud size of 75 km. More recent unpublished studies using lidar data have indicated a size

even smaller than this. For the assumption of horizontal homogeneity to be valid, the cloud should be homogeneous and uniform for a major part of the tangent path through the relevant part of the atmosphere (see Figure 3.3.1), typically several hundred kilometers. This is clearly not the case, even for the higher altitude cloud that SAGE II and SAGE III most readily detect. Simulation studies show at least three significant effects of the inhomogeneous nature of cloud on the solar occultation data. The first is that there may be an error in the identified cloud altitude. For example, if cloud occurs to one side of the tangent point, as shown in Figure 3.3.1, it will be assigned to the tangent altitude, which is less than the true altitude. In addition, because of the flattened shape of much high altitude cloud, the ray path through such a cloud will be less than if it had occurred at the tangent point. This will result in a lower apparent extinction. A third problem that occurs is to the inverted extinction value just below the cloud. The inversion scheme assumes that the cloud is uniform along the ray path and that any ray path whose tangent point is lower than that at which the cloud is detected must pass through the cloud. This is often not the case if the cloud is non-uniform or small and isolated. Inverted values for lower altitudes, particularly those just below the cloud, will be too low and may sometimes even be negative (Note: This is true only in respect of a downward, onion peel inversion scheme. The iterative Twomey-Chahine approach suppresses the negative values).

Some problems may also arise because of vertical cloud inhomogeneity. The vertical resolution of the aerosol/cloud extinction profile for SAGE III will be 0.5 km, which corresponds approximately to the size of the viewing slit. If the vertical extent of a cloud embedded in this profile is less than these values, some unattenuated solar radiation will be received at the satellite instrument even if the cloud is in the centre of the field of view. The detected signal is an integration over the complete instrumental field of view. Although this signal will show attenuation, the amount of attenuation will not correspond in any simple manner to that actually produced by the cloud. (See Appendix B. for further discussion of the inhomogeneity problem and the potential use of individual scans to give information about the presence of inhomogeneities).
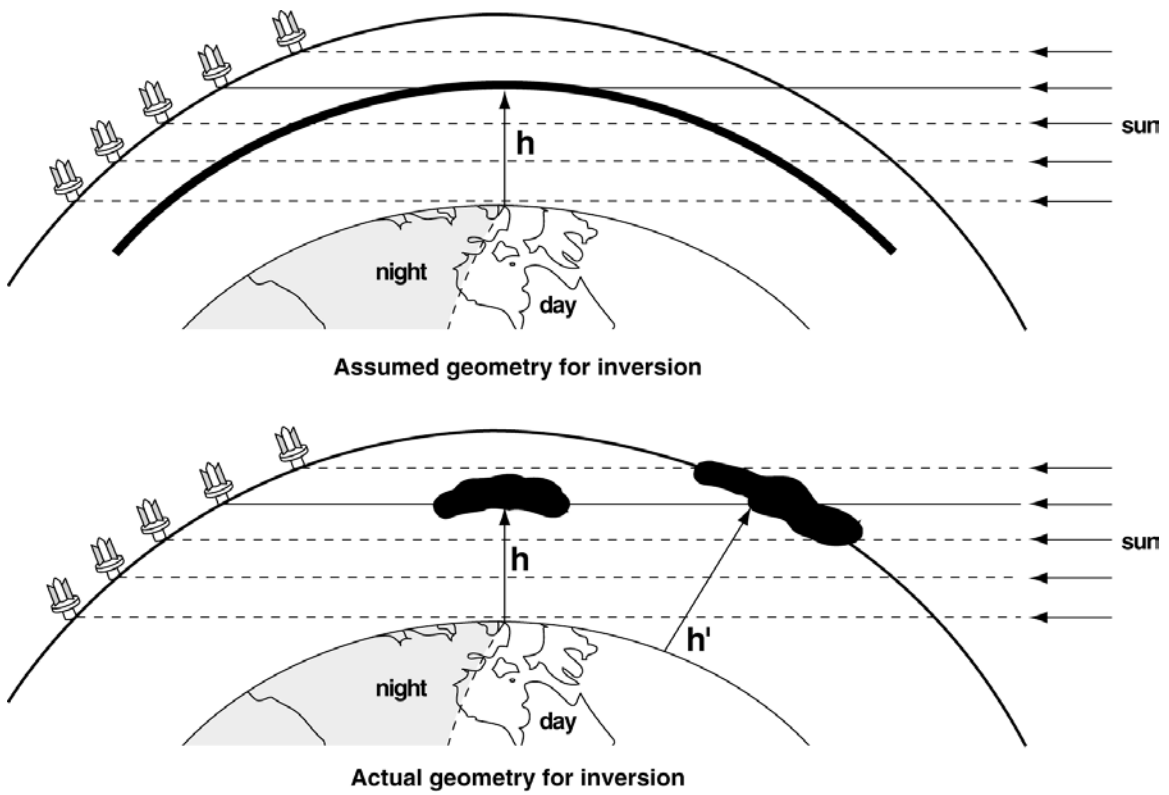
Figure 3.3.1 Schematic showing the SAGE III ray path and the way in which a cloud may be present at the tangent point or to one side of this point.

3.4 Input Data Requirements

The input data needed for the determination of cloud presence in each event will consist of vertical profiles of aerosol extinction, together with their estimated errors, at wavelengths of 525 nm, 1020 nm, and 1550 nm. It is assumed that the data are supplied at vertical intervals of 0.5 km and that missing data are shown by an identifiable fill value. In order for cloud data processing to be initiated for any event, at least one extinction value, together with its error bar must be present simultaneously at all wavelengths, at an altitude of 30 km or lower. Data for altitudes below 6 km will not be processed by the present algorithm, but space will be left in the output arrays for the results of possible future processing of these low altitude data.

The input data just described will be available as part of the normal data processing stream and are sufficient to determine all elements, except one, of the output data format described in Section 3.5.1. The indeterminable element is index value 4 of the cloud uncertainty index profile. This index value indicates that atmospheric conditions are such that the wavelength extinction characteristics of the aerosol are too close to that of cloud for the defining algorithm to work satisfactorily. The most notable conditions under which this will occur are those following volcanic injection. Such information may be available at the time that the event occurs but is more likely to become available at a later date. This would be as a result of observations and measurements made by other persons and instruments and from analysis of trends in the SAGE III aerosol extinction data over an extended period of time.

3.5 Output Data Descriptions

The general characteristics of the SAGE III cloud data products are described in the following sections.

3.5.1 Cloud Presence Data

The basic product will be a vertical profile extending from 0 to 30 km containing cloud presence information at 0.5 km intervals, plus two similar profiles, the first giving uncertainty information and the second containing a cloud area index. The altitude range has been chosen to extend over all altitudes at which this, or future modifications of this, algorithm are likely to be able to identify the presence of cloud. If future modifications of the algorithm are able to identify PMCs, these will be listed separately.

The **cloud presence information** will be given by an index at each altitude whose value will be set as follows:

0 insufficient input data (i.e., data missing for at least one aerosol wavelength)
1 no cloud present - under all aerosol conditions

2 no cloud present - should not occur under background aerosol conditions, ambiguous under moderate to intense volcanic aerosol conditions

3 cloud present - should not occur under background aerosol conditions, ambiguous under moderate to intense aerosol volcanic conditions.

4 cloud present - under all aerosol conditions

This method of indexing follows the discussion given in Section 3.2.3 and, in particular, the information given in Figure 3.2.7 and Table 3.2.3.

The **uncertainty information** will be given by indices as follows:

0 insufficient input data

1 The limits of error attached to the aerosol extinction values used in the algorithm are such that the determination of the cloud presence index value can be made with confidence.

2 The limits of error attached to the aerosol extinction values used in the algorithm are such that the determination of the cloud presence index value cannot be made with confidence.

3 Data location on the profile (e.g., a data point located below a strong but not opaque cloud layer) is such that the determination of cloud presence cannot be made with confidence.

4 Atmospheric conditions are such (e.g., volcanic aerosol present) that the wavelength extinction characteristics of the aerosol are too close to that of cloud for the algorithm to work satisfactorily.

It should be noted, as explained above in Section 3.4, that it will not be possible to complete the uncertainty information when an event is first processed if this is close to the time of the actual event. Information on volcanic contamination may only become available later as a result of other observations and/or examination of long-term trends in the aerosol extinction. For this reason, we propose to have a single **quality assessment flag** for each event. This flag will initially be set to **0** when the event is first processed. At a latter stage when atmospheric and other factors affecting the uncertainty in the determination of cloud presence have been evaluated, this flag will be set to **1** and the uncertainty indices reset where necessary. Reprocessing of the input data will not be required.

The cloud area index is a four digit number that shows the regions of the plot (as in Figure 3.2.7 and Figure 3.6.2) over which the error ellipse extends. An index of 0230 signifies that the ellipse extends over regions 2 and 3 of these plots, an index of 1200 signifies that the ellipse extends over regions 1 and 2. The index is assigned for all non-zero values of the cloud uncertainty flag, it takes a value of 0000 if there is insufficient or non-physical input data.

3.5.2 Other Higher Level Data Products

In addition to the basic cloud presence data described above and the browse data discussed in Section 3.5, it may be possible to produce higher level data specifically related to polar stratospheric clouds and polar mesospheric clouds.

Polar Stratospheric Clouds

The cloud presence algorithm just described is based on the premise that the cloud particles are large relative to the measurement wavelengths and, hence, that the aerosol extinction coefficients measured by SAGE III will vary little spectrally. With regard to the identification of PSCs, the algorithm should work reasonably well with Type 2 clouds, which are thought to be predominantly water ice clouds with reasonably large particles (though probably smaller than those typical of upper tropospheric cirrus). However, performance of the algorithm will be problematical for Type 1 (HNO_3-H_2O) PSCs, regardless of their exact composition. The available condensable nitric acid supply is some 500 times smaller than that of water vapor, meaning that Type 1 particle sizes will likely be in the same range as the SAGE III aerosol channel wavelengths. Therefore, without considerably more information, it may be difficult to routinely separate Type 1 PSCs from aerosols with any confidence.

As stated in section 2.2, there are still outstanding uncertainties with regard to the composition and reactive efficiency of Type 1 PSCs and to the details of the denitrification process. In this regard, desirable higher level data products to be derived from SAGE III would include:

Identification of Type 1 PSCs The following factors may allow the detection of Type 1 PSCs: wavelength dependence of extinction; increase over background of the absolute extinction; or greater spatial homogeneity than Type 2 PSCs. Initially such analysis will be done off-line, but at some later point it may be possible to include this into the routine processing.

Particle surface area of PSCs This is particularly of interest in the Arctic, where the frequency of PSC occurrence is much lower than in the Antarctic, making the knowledge of surface area available for catalyzing heterogeneous chemistry more crucial. An issue to be settled is the refractive index to be used for Type 1 PSC particles. Type 1 PSCs may be embedded in the background aerosol ensemble; surface area would then be a higher level aerosol product.

Simultaneous PSC extinction coefficient and temperature measurements This pair of observations, if done with sufficient resolution and accuracy, might lead to considerable insight into the composition and formation mechanisms of Type 1 PSCs. For example, the behavior of extinction coefficient with temperature should be vastly different for nitric acid trihydrate - an abrupt phase change, hence increase in extinction - than for a

supercooled ternary (H_2SO_4-H_2O-HNO_3) solution droplet - a more gradual uptake of HNO_3, hence a gradual increase in extinction with decreasing temperature.

Polar Mesospheric Clouds

To detect the presence of PMCs, the SAGE III transmission data for the short wavelength aerosol channels (385 and 521 nm) between 70 and 95 km will be screened for the presence of layers of attenuation above the expected Rayleigh scattering background. After the layers are detected in those two aerosol channels, the other wavelength channels will be used to obtain the wavelength dependence of the PMC attenuation. For all the SAGE III wavelengths, except for the ozone absorption around 290 nm and the oxygen A-band absorption from 759 to 767 nm, the PMC extinction at altitudes of 80 to 85 km will be much larger than the residual molecular absorption at those altitudes.

Because of the small sizes of the PMC particles as discussed in Section 2.3, it is expected that the aerosol/cloud separation technique discussed in Section 2.3 would in fact identify PMCs as aerosols. However, given it is believed that the aerosol attenuation at those altitudes is negligible in absence of PMCs, any "aerosol" layer identified above 70 km is likely to be a PMC layer (Thomas, 1989).

To detect the presence of PMCs, the SAGE III transmission data for the short wavelength aerosol channels (385 and 450 nm) between 70 and 95 km will be screened for the presence of layers of attenuation above the expected Rayleigh scattering background. At these two wavelengths the contributions of molecular absorption can be expected to be negligible above 70 km. The Rayleigh scattering background can be calculated from the atmospheric density determined from the oxygen A-band measurements, with a small correction for the fact that oxygen is not uniformly mixed above 80 km.

After subtracting the molecular scattering contribution the residual optical depth at 385 and 450 nm can be expected to be zero plus any contribution due to the presence of PMCs. So the detection of PMCs will be essentially the detection of positive deviation above the measurement noise. A threshold of 5 times the RMS noise should be sufficient to eliminate most false positives, [about than 1 in 7 years of SAGE III measurements, assuming Gaussian statistics]. Most PMC layers will produce measurable optical thicknesses in several adjacent altitude bins [Debrestian *et al*. 1997a and 1997b], and will be seen at both 385 and 450 nm. These properties can be used to reduce the detection threshold, by requiring that the positive signal be detected in two or three adjacent $\prod$ km altitude bins and/or both wavelength channels. Although to use this latter approach, the "noise" statistics must be analyzed to verify that there is no correlation of the "noise" between adjacent altitude bins or in different wavelength channels.

After the layers are detected in those two aerosol channels, the other wavelength channels will be used to obtain the wavelength dependence of the PMC attenuation. For all the SAGE III wavelengths, except for the ozone absorption around 290 nm and the oxygen A-band absorption from 759 to 767 nm, the PMC extinction at altitudes of 80 to 85 km will be much larger than the residual molecular absorption at those altitudes.

Because of the small sizes of the PMC particles as discussed in Section 2.3, it is expected that the aerosol / cloud separation technique discussed in Section 2.3 would in fact identify PMCs as aerosols. However, given it is believed that the aerosol attenuation at those altitudes is negligible in absence of PMCs, any "aerosol" layer identified above 70 km is likely to be a PMC layer (Thomas, 1989).

3.5.3   Browse Data

The principal component of the browse data will be a set of cloud occurrence images similar to those presently produced from the SAGE II data set. Data points corresponding to individual SAGE III events will be accumulated over a season (DJF, MAM, JJA, and SON) at 1-km intervals between 6 km and 30 km. Cloud occurrence (defined as the ratio of the number of cloud events to the total number of events) for each altitude will be determined within specified latitude-longitude bins and used to create contour maps of cloud occurrence. Similar maps will be produced at a number of standard pressure levels (300, 200, 150, 100, 70, 50, 30 hPa). The latitude-longitude bins have still to be defined; those used for SAGE II data are 45° longitude by 10° latitude. A minimum number of events will be required to occur within a bin for the cloud occurrence to be defined. Associated maps will be available showing the event density at each altitude. By using binomial statistics, confidence limits may be estimated for the cloud occurrence at any point. An example of a browse map produced from SAGE II data is given in Figure 3.5.1. This figure shows the SAGE II cloud coverage for the time period September-November, 1986, at an altitude of 14.5 km. Data gaps over the Indonesian region are due to the obscuring effects of higher altitude cloud, which is particularly frequent in this region.

In addition to the browse maps, it will be possible to access individual events by time, location, or by reference to the browse maps. The vertical profiles of extinction at 521, 1020, and 1540 nm may be viewed (as in Figure 3.1.3) so that the type of event (no cloud, transparent cloud, or opaque cloud) may be determined visually. It will also be possible to display the event against the background of the theoretical wavelength relationship and cloud presence determination scheme (including error bars), as shown in Figure 3.6.2. A further development will be to provide a similar display showing the distribution of a selected group of data points (e.g. all data within a specified area or within a given bin) against the same background. In this way the viewer may judge the effectiveness of the algorithm and the wavelength behaviour of a particular data ensemble.
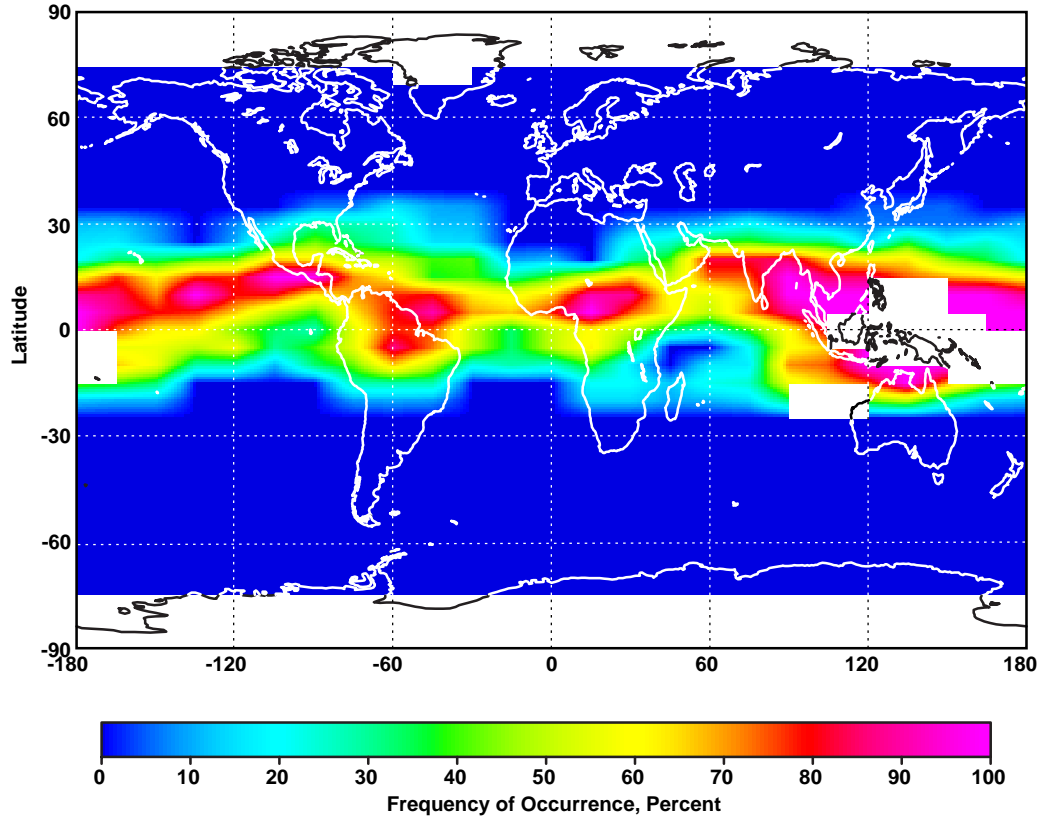
Figure 3.5.1 An example of a browse map produced from SAGE II data. The data shown is for the time period September-November, 1986, at an altitude of 14.5 km. Data gaps over the Indonesian region are due to the obscuring effects of higher altitude cloud

3.6   Formulation of the Cloud Presence Algorithm

The flow chart for the main processing sequence is shown in Figure 3.6.1. It is a subset of that for the total data processing sequence given in Figure 3.6.3. (The flow chart for another subset, the quality control procedure is shown in Figure 3.10.1). The objective of the main processing sequence is to examine the aerosol extinction data for each event in turn , test for the presence of cloud, assess the reliability of the test result and set the cloud presence index (PRndx) and the cloud presence uncertainty index (UNndx) at each altitude. At the time of initial processing there may be insufficient information available to make a reliable assessment of the uncertainties. The quality control flag (QUflg) for each event will be set to zero. At a later stage, when a better assessment of errors can be made (in particular that relating to volcanic activity), the uncertainty indices will be revised and the quality control flag reset to unity. This will be discussed in Section 3.10. The stages in the processing sequence are as follows:

45

1) <u>Event/data selection</u> It is expected that processing for cloud presence will occur as part of the main processing sequence and will be handled one event at a time. The input data needed consists of the aerosol extinction profiles at 521, 1020, and 1540 nm together with their error bars. At this point the quality control flag for this event is set to zero.

2) <u>Set indices for altitudes 0-6 km</u> The present algorithm will not process data below 6 km. In order to allow for possible future extensions that will allow processing to lower altitudes, the output profiles containing the cloud presence indices and the uncertainty indices extend to zero altitude. Values in the profiles for altitudes less than 6 km are set to zero.

3) <u>Sequential data processing</u> Data processing is carried out sequentially by decreasing altitude, commencing at 30 km and terminating at 6 km.

4) <u>Test for the presence and nature of the data at each altitude</u> The existence, the physical reality and the logical consistency of the data is checked at all three wavelengths and at each altitude. If the input data exist but are physically unrealistic (e.g. negative values of extinction) or logically inconsistent (e.g. variances and covariances mathematically incompatible) further processing at the current altitude ceases and passes to the next altitude for this event. If there is either consistent data or fill values, processing goes to the next stage. The processing sequence followed then depends upon whether data are present or not, whether it is present at all three wavelengths and whether the current altitude is the maximum altitude under study (30 km) or lower.

  If data are not present at all three wavelengths,
   - If the altitude is the maximum (30 km), it follows that there are no useful data for this event. The cloud presence indices and the uncertainty indices are set to zero at all altitudes and processing goes to the next event.
   - If the altitude is not the maximum, and data are absent at all three wavelengths, it is assumed that this is due to the presence of cloud at the altitude under study. The cloud presence index is set to 4 at this level. Both cloud presence and uncertainty indices are set to zero at all lower altitudes. Processing goes to the next event if data are present at one or two wavelengths only, the situation is regarded as indeterminate and the cloud presence and uncertainty indices are left set to zero. Processing goes to the next event.

  If data are present at all three wavelengths,
      The test procedure described in Sections 3.2.2 and 3.2.3 is carried out to determine whether cloud is present or not and to set the value of the cloud presence index. This procedure is defined in more detail below. Error bars on the aerosol extinction values are examined to assist in the setting of the uncertainty indices. This procedure is described in Section 3.6.1. Processing goes to the next lower altitude; when all altitudes above 6 km have been processed, processing goes to the next event.

The cloud presence test itself is based upon Figure 3.2.7. The input variables are the ratios (at each altitude) -

$$x = 1020 \text{ nm aerosol extinction} / 1540 \text{ nm aerosol extinction}$$
$$y = 525 \text{ nm aerosol extinction} / 1020 \text{ nm aerosol extinction}$$

The parallelogram areas in that figure are bounded by straight lines joining the four vertices - (0.8, 1.0), (0.8, 2.5), (xtc, 2.5) and (xcc, ycc). There are three parallelograms corresponding to different values of xtc, xcc, and ycc. The cloud presence index is set to 4, 3 or 2 depending upon where the data point lies within these three areas. If the data point lies outside all the parallelograms, then the index is set to 1.
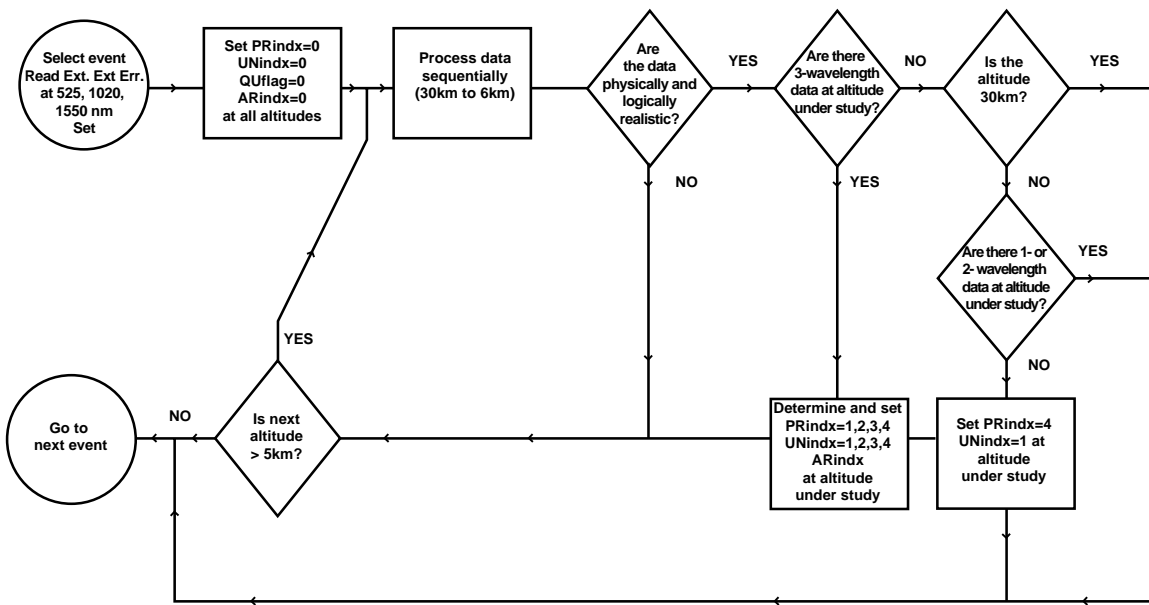
Figure 3.6.1 Flow chart for the main processing sequence.

3.6.1   Uncertainty Estimates

Alternative values for the cloud uncertainty indices are listed in Section 3.5.1. The indices do not supply quantitative uncertainties but are simply indicators of the reliability of the determination of cloud presence. The setting of the uncertainty index to zero for the case of insufficient input data has already been described in Section 3.6. This case is not subject to further revision unless the input data change. The setting of an uncertainty index to the value 1, 2, or 3 is made on the basis of internal information about the aerosol extinction values, either at the altitude in question or from neighboring altitudes. Setting a index to the value 4 is made on knowledge of the statistical behaviour of a much larger data set or from external information on atmospheric conditions (notably changes due to recent volcanic eruptions). At the time of initial processing, the information necessary to set the index to a value of 4 may be incomplete. As a consequence the uncertainty indices

will be revised at a later stage and the quality control index reset. The dominance order of index values is 0, 4, 3, (2 or 1). The initial setting of an uncertainty index value is made as follows:

- The uncertainty index is set to 0 if the data set is incomplete.
- If the data set is complete but there is reason to believe that volcanic or other contamination is present, the uncertainty index is set to 4.
- If the altitude of the datum under test is below a strong cloud layer, the uncertainty index is set to 3. The conditions under which a index will be set to this value are still under study and will be the subject of data simulation tests. Information now available indicates that data obtained less than 3 km beneath a strong but not opaque cloud layer may show erroneous extinction values.
- The uncertainty index is set to 1 or 2, dependent on the magnitude of the error bars attached to the input wavelength extinction values. The procedure is illustrated in Figure 3.6.2. The error estimates attached to each extinction value are used to calculate errors for the ratios (525 nm extinction / 1020 nm extinction) and (1020 nm extinction / 1550 nm extinction). These ratio errors are shown as error bars in Figure 3.6.2 and used to draw the error ellipse shown. The positions of the error ellipse is determined in relation to the areas used to distinguish cloud from aerosol data points. If any part of the error ellipse crosses one of the lines shown in bold in the figure, the uncertainty index is set to 2; if this does not occur, the index is set to 1. This procedure ignores the left-hand and upper edges of the parallelograms, which are shown by regular lines. These edges are not critical to the resolution of cloud from aerosol. The error ellipse has as major and minor semi-axes the error bars themselves. The error ellipse is also used to define the cloud area index as detailed in Section 3.5.1.
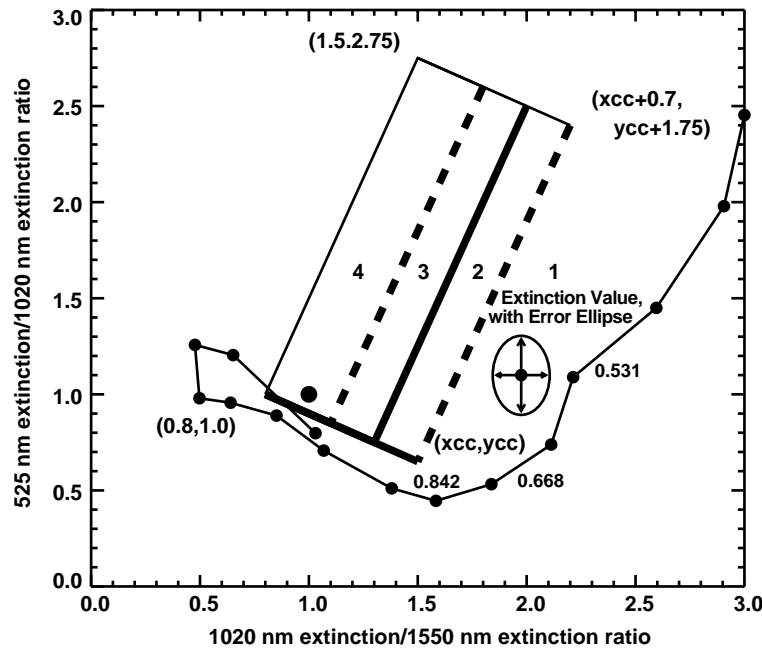
Figure 3.6.2 Illustration of the dependence of the uncertainty index upon the magnitude of the error bars. The parallelogram edges shown in bold are used in the setting of the uncertainty index. If any part of the error ellipse crosses one of these edges the uncertainty index is set to 2. The uncertainty index is otherwise set to 1.

3.6.2   Data Processing Sequence

The total cloud data processing sequence is given in Figure 3.6.3. It consists of the following blocks

Main Processing Sequence (discussed in Sections 3.6 and 3.6.1) This will take place as part of the standard inversion procedure and be carried out sequentially event by event. Of necessity, determination of cloud presence must follow the inversion for the multi-wavelength aerosol extinction. Preliminary values of the uncertainty indices will be set during main processing, definitive values will be set later as a part of quality control.

Data Accumulation (discussed in Section 3.10) Cloud and aerosol data will be accumulated on a monthly basis for use in quality control.

Quality Control (discussed in Section 3.10) The monthly data accumulation will be used to produce gridded cloud and aerosol maps. These will be used in conjunction with external data on sudden events such as volcanic eruptions, data from other instruments, and previous SAGE III data, to assess the data quality for the current month. A quality control instruction file will be produced.

<u>Uncertainty Adjustment (discussed in Sections 3.6.1 and 3.10)</u> The uncertainty information for the current months data will be reset where necessary, and a new set of data files for archival and public release prepared.
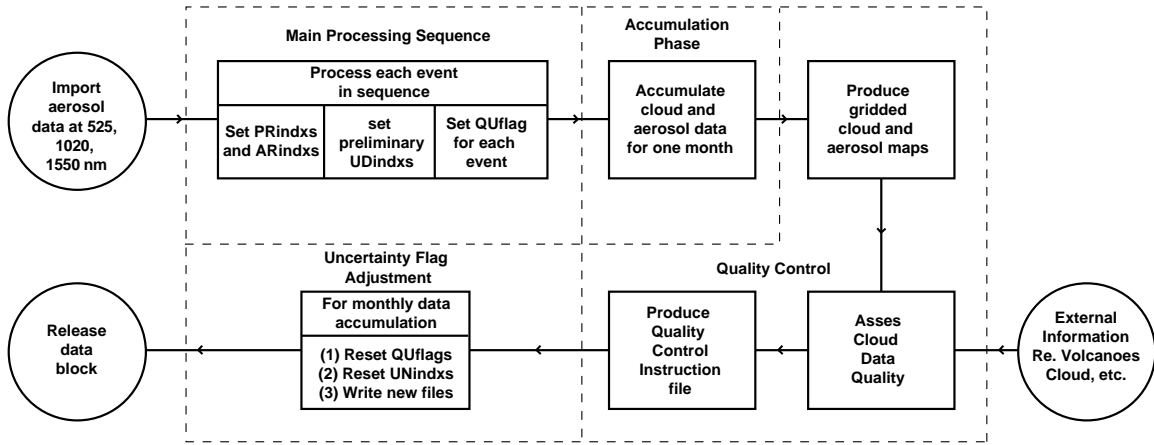
Figure 3.6.3 Flow chart for the entire cloud processing sequence.

3.7 Numerical Considerations

No special numerical considerations apply. The data processing required is extremely simple and not likely to cause numerical problems. In the event that the extinction values passed to the cloud algorithm are unrealistic (e.g. zero or negative), it is provisionally assumed that the associated error bars will be large enough to cause the data point in question to be identified as unreliable according to the procedure described in Section 3.6.1.

3.8 Algorithm Testing Requirements

Algorithm testing will depend for the most part on the development of detailed model atmospheric scenarios that include cloud, followed by the simulation of the SAGE III transmission profiles, the inversion to produce the aerosol profiles needed as input to the cloud presence algorithm and the operation of this algorithm. The output products, e.g. the cloud presence information and the uncertainty indices, are then to be compared to the input model. It is not possible to consider this operation in isolation. The cloud presence algorithm utilizes the aerosol product and is dependent upon the successful operation of the aerosol inversion algorithm in the presence of cloud. Successful testing of that algorithm for non-cloud situations will not however guarantee its success under cloudy conditions. The essential difference lies in the limited structure size of cloud, requiring the creation of a detailed two-dimensional model (altitude and horizontal distance) for the cloud and aerosol, and the simulation of the SAGE III raypath for appropriate tangent altitudes and locations through this inhomogeneous mixture.

The best source of input data for the model simulations are the continuous backscatter records now available from airborne and satellite lidar. These backscatter data may be converted to extinction by application of a simple model and added to the extinctions due to aerosols and molecular constituents. Data are available covering all latitudes and most cloud types from tropical cirrus to polar stratospheric clouds. Models will have to be developed to cover a wide range of cloud types, optical depths and locations relative to the SAGE III tangent positions. Varying amounts of background aerosol will also have to be included into the models ranging from background conditions to heavy volcanic/dust cloud and pollution conditions appropriate to the altitude regime under study. This proposed simulation resembles that described in Section 3.2.2, with the inclusion of the inhomogeneity problem discussed in Section 3.3. It is potentially of considerably more complexity, allowing for the inclusion of such additional features as the instrument scan cycle and the satellite movement, as well as the problem of separating the extinction due to aerosols and cloud from that due to the gaseous absorbers. Some simulation is currently ongoing, utilising tropical high cloud data from airborne and satellite lidar. The objective of this work is to study the effects of cloud inhomogeneities on the SAGE II extinction, with a view to interpreting the SAGE II cloud extinction distribution.

Algorithm performance will be studied for increasingly difficult scenarios, commencing with the simplest case of uniform thin cloud against a background aerosol. Following successful testing of simple cases, higher extinction volcanic/surface derived aerosol may be added into the model and the cloud allowed to become inhomogeneous. In this way it will be possible, not only to validate the algorithm but also to assess its performance under different atmospheric scenarios. This information will in turn be used as an aid in the setting of the uncertainty indices for different atmospheric situations as well as a guide to improvements in the algorithm.

In order to establish continuity of the SAGE III cloud data with that from SAGE II, it is highly desirable that, following the launch of SAGE III, at least part of its data be parallel processed with the current SAGE II algorithm. The latter is based on the use of aerosol extinction at 525 nm and 1020 nm only. Following the discussion in Section 3.2.2, it is anticipated that the SAGE III and SAGE II algorithms should agree in a non-volcanic atmosphere. Increasing divergence is to be expected as volcanic contamination increases. This intercomparison will be particularly necessary if the cloud data are to be used to study long-term changes such as those connected with the ENSO cycle.

3.9   Data Product Validation Plan

The data validation plan will consist of two major subdivisions: planned measurements by direct and remote sensors on a single event basis, and intercomparisons with data from other sensors on a statistical or target of opportunity basis. The validation of the aerosol retrieval is of course central to cloud detection, and this component is covered in the SAGE III validation plan. Here we concentrate on the validation of the cloud presence data product.

3.9.1   Planned Field Measurements

Clouds in the Middle and Upper Troposphere

There is an extensive program of field measurements planned for the validation of SAGE III aerosol measurements (see SAGE III validation plan). This program is based on the successful field campaigns carried out for SAGE II aerosol measurements. It includes measurements by in-situ and remote sensors placed on the ground and on aircraft, balloons, and rockets. The proposed instruments include lidar, photometers, other optical instruments, particle collectors and optical particle sensors. Cloud characterisation instruments will also be flown. It seems logical that any cloud validation field program should be integrated with that for aerosols and where feasible this will be done.

SAGE II was not specifically designed for cloud studies and cloud validation was not included as part of the overall validation program. The only published direct comparisons of cloud observed by SAGE II with that found as a result of a field program was reported by Kent *et al*. [1993]. Cloud and aerosol measurements were made by airborne lidar near the west coast of the USA where the lidar system was used to underfly the SAGE II optical paths for four different events. The basic problem of cloud validation as opposed to that for the other SAGE II and SAGE III measurements is the inhomogeneous nature of cloud and its small structure size as compared to the length of the raypath through the atmosphere. The situation is further complicated by fairly rapid (as compared to a typical aircraft flight duration) changes that can take place within a cloud. To completely validate the SAGE III algorithm for cloud presence, it would be necessary to measure instantaneously the optical properties of the atmosphere along a vertical section of the atmosphere extending the total length of the raypath. In order to understand and interpret the satellite measurements in terms of the radiative impact at other wavelengths, or to use the data to provide a measure of water content, it is also desirable to make microphysical measurements within the cloud at all altitudes and locations under the raypath.

These measurement requirements just described are clearly impossible to satisfy. The instrument that comes closest to achieving them is downward looking lidar from a platform above the cloud. Successful airborne lidar measurements were made as part of the LITE validation program [Schreiber *et al.,* 1995]. Downward looking airborne lidar observed inhomogeneous cloud structures similar in detail to those seen from space. Provided the location of the raypath can be accurately specified (to 10 km or better) in advance it is clearly possible to use an airborne system to observe the same cloud as that seen from space. The Aerosol Research Branch at NASA/LaRC possesses an airborne lidar system that has previously been used to make upward looking measurements of cloud and stratospheric aerosols. This can easily be modified to make downward measurements from the NASA DC-8 aircraft. The ceiling altitude of this aircraft is about 40,000 ft which would not permit the downward-looking observation of tropical cirrus cloud. For such measurements consideration will be given to using a smaller lidar system

onboard the NASA ER-2 aircraft or other high altitude platform (e.g., NCAR WB-57). Alternatively the DC-8 based lidar system may be used somewhat less satisfactorily in the upward looking mode for validation measurements on tropical high cloud.

Lidar data will be supplemented by in-situ measurements made within high cloud (ice-water content, particle size distribution, temperature etc.). These measurements should be made within the same cloud as that observed by SAGE III and the airborne lidar. Where possible the vertical and horizontal structure will be probed. Consideration will also be given to making radiometric measurements of the sun from within and through the top of the cloud from without, in order to simulate the SAGE III measurement directly, as well as to provide a link between the radiative and the microphysical properties of the cloud. Cloud photography from high and low flying platforms will form an integral part of the validation program. Data from two forms of camera are potentially useful. The first is an all-sky camera to be mounted so as to observe cloud structure close to and on either side of the flight path. When improved post-flight ephemeris information becomes available, more accurate cloud simulations can then be carried out. This camera needs to be located on the aircraft in an upward looking bubble and its operation would be automatic during a data take. The other camera would be a calibrated digital instrument looking directly at the sun (through suitable filters) with a long focus lens. This would enable high resolution measurements of the intensity distribution across the solar disk to be made, similar to those made by the SAGE III instrument. These images are invaluable for the understanding and interpretation of the scan intensity distribution under cloudy conditions.

An alternative to lidar is the use of microwave remote sensing to determine cloud structure. The University of Wyoming KingAir combines a 95 GHz 'KESTREL' radar with in-situ probes allowing direct observations of cirrus crystals at the same time as the entire vertical structure of the cloud is depicted. The KingAir has a maximum operating altitude of about 10 km, and the radar has a useable range (high enough sensitivity) to about 3 km above the flight altitude. The radar can be operated with a horizontal beam as well to depict the horizontal uniformity of the cloud, a feature not at present available to the lidar. The KESTREL radar provides a reflectivity image with 30 m resolution above or to the side of the flightline. The 2D imaging probes provide a direct measure of geometric cross-section, which then directly yield the horizontal-path optical extinction coefficient. Data already in hand show that the extinction coefficient and the radar reflectivity are correlated, and that the radar has sufficient sensitivity to detect clouds producing extinction values in the range of SAGE III detectability. The correlation is dependent on crystal type, but is expected to be fairly conservative for cirrus crystals. In-situ probes on the KingAir also provide total ice water content, crystal size distribution, and state parameters; these complement the primary measurements and provide further help in interpretation and modeling of cirrus processes.

Clouds and Aerosols in the Lower Troposphere

In the lower troposphere (<7 km) validation of both the SAGE-III aerosol and cloud algorithms can be carried out by direct comparisons with in-situ measurements. For this

purpose we plan to utilize the University of Washington's Convair C-580 research aircraft. The C-580 is equipped with comprehensive instrumentation for aerosol and cloud characterisation through in situ measurements. Moreover, it can be deployed at short notice in order to document unpredictable events (e.g., volcanic eruptions, large dust storms, forest fires, etc.) that will provide verification data for a wide variety of geophysical situations.

The instrumentation aboard the C-580 can provide aerosol size spectra from 0.02 to 50 μm diameter, aerosol total scattering and backscattering, light coefficients at 550 nm and 700 nm, aerosol mass concentrations, aerosol composition, aerosol shape, the effect of humidity on particle size, cloud condensation nucleus spectra, and (for very polluted conditions) the light absorption coefficient of the aerosol.

In-cloud measurements aboard the C-580 include cloud and precipitation liquid water content, the complete size spectra of cloud and precipitation particles, particle phase (liquid water or ice), ice crystal habits, the angular distribution of scattered solar radiation in the cloud, as well as cloud base and cloud top heights and temperatures.

Polar Stratospheric Clouds

The NASA LaRC Aerosol Research Branch airborne lidar system has been used quite successfully in many past missions focused on the scientific study of PSCs [Kent *et al.,* 1986; Poole *et al.,* 1988; McCormick *et al.,* 1990]. Measurements with this system were the first to delineate Type 1 and Type 2 PSCs [Poole and McCormick, 1988] and to characterize their optical backscatter properties [Kent *et al.,* 1990] and evolution [Poole *et al.,* 1990] in detail. There has been no airborne mission to date aimed at validating satellite PSC retrievals, although there were several nearly simultaneous measurements with SAM II during the 1989 Airborne Arctic Stratospheric Expedition (AASE) I (Osborn *et al.,* 1990). These authors found good comparison between the lidar and SAM II well inside the edge of a spatially homogeneous PSC, but relatively poor comparison near the edge of a PSC due to the inherent spatial and temporal variability.

Upward-looking airborne lidar measurements along the solar raypath will be very useful for validating SAGE III PSC measurements. The LaRC system could be used aboard the NASA DC-8; flights at relatively high altitudes (>35,000 ft) are recommended to minimize difficulties of penetrating cirrus with the lidar. Correlative measurements in both the Arctic and Antarctic would be very useful, but logistics and cost may restrict flights to the Arctic. Dual-polarization backscatter measurements at (at least) one wavelength are required to examine particle phase. Additionally, multi-wavelength scalar backscatter measurements are desirable to provide some information on PSC particle size.

The lidar measurements should be supplemented by in situ measurements within the PSCs, which would require the use of balloons or a high-altitude aircraft such as the NASA ER-2 or the NCAR WB-57. These measurements might include two-wavelength in-situ backscattersonde; particle size distributions; particle composition, either by some

direct means or indirectly using an instrument like the NCAR Multi-Angle Scattering Probe; total particle (CN) counts; temperature; and mixing ratios of condensables (HNO_3 and H_2O).

Possible Flight Scenarios

The minimum requirement for the determination of cloud structure useful for SAGE III validation would be to underfly the raypath over a distance of at least two hundred kilometers about the tangent location, this distance being chosen to correspond to the maximum length of the raypath within a 1 km spherical shell. It is also necessary to know the location of the raypath in advance to an accuracy of 10 km or less, a distance less than the typical horizontal dimension of a high altitude cloud. A possible flight pattern suitable for the validation of high altitude tropospheric cloud is shown in Figure 3.9.1. The event is assumed in this case to be a sunset and the approximate altitude of the highest cloud is determined from ancillary data and from a limited number of lidar measurements made immediately prior to commencement of the validation flight. The flight track ABCDEF is as drawn (the curvature of the earth is exaggerated in this figure), the first leg being made at altitude the altitude of the highest clouds to determine in-situ characteristics (particle size, temperature, water content) and to make radiometer and video camera measurements looking back towards the sun. The flight is timed so that the aircraft arrives at the descending leg CD at the time of the actual SAGE III event. Radiometer and video images of the sun showing cloud can then be made at this critical time from a range of flight altitudes. Following the event the return leg (DEF) is made beneath the raypath using upward looking lidar to observed the cloud macrostructure. Total flight time will be of the order of 30 minutes dependent upon aircraft speed.

An alternative scenario applicable to the validation of high altitude clouds or PSCs at high latitudes, such as might be observed by SAGE III onboard the METEOR spacecraft, would be to follow the terminator. At 60°N the terminator moves at a velocity of the order of 800 km per hour, similar to that of a jet aircraft. In situ measurements of PSCs would not be possible from a normal aircraft but lidar, video camera and radiometer measurements would be. A flight track around the pole at constant latitude could be chosen so that video and radiometer measurements could be made towards the sun continuously, together with upward looking lidar measurements. In this way, the distribution in altitude and longitude of the clouds could be determined, while the aircraft passes through the subtangent points of each event approximately every 100 minutes. Continuous measurements made in this way would be very valuable for the simulation of the SAGE III events covered.
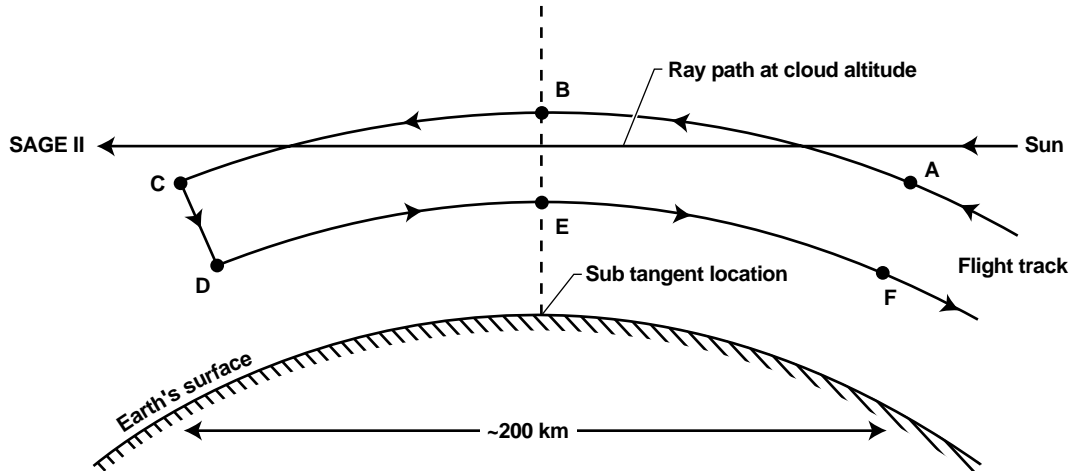
Figure 3.9.1 Possible scenario for a cloud validation flight. The flight track is shown by ABCDEGF. The outward flight, during which in situ measurements are made, is flown at cloud top altitude prior to the event time. At the event time the aircraft descends to a lower altitude while taking video images and radiometer measurements of the sun. During the return flight upward looking lidar measurements are made of the cloud.

3.9.2   Data Intercomparisons

Tropospheric Clouds

An important part of the validation program will be to make comparisons between individual SAGE III profiles and average cloud occurrence rates with those from other on-going programs and observations. Overlaps between SAGE III and other satellite retrievals (e.g., ISCCP, HIRS) will be exploited for cloud presence/absence consistency [e.g., Liao *et al*., 1995a, 1995b]. Many targets of opportunity will likewise exist for comparisons with ground-based and radiosonde data (see, for example, Smith and Platt, 1978). In addition, pilot reports of cloud cover (PIREPS) are routinely archived at the National Center for Atmospheric Research, and could provide a valuable data source for more direct in situ determinations. With a combination of global observations from other satellites, and ground-based and in situ comparisons from radiosonde and pilot observations, the ability of SAGE III algorithms to properly identify the presence of clouds should be accurately assessed. Consideration will be given to the possible use of the considerable database of surface cloud observations taken by lidar systems in various parts of the world. Space-borne lidar measurements similar to those from LITE [McCormick *et al*., 1993b] will also be very valuable, not only to the statistics of the SAGE III cloud measurements, but also to the interpretation of the data themselves. These lidar and other measurements will enable us to determine whether SAGE III data are simply to be used as a measure of overall cloud occurrence or whether they can be used to distinguish between various cloud types. They may assist in the possible quantitative interpretation of the data in terms of ice water content or radiative impact.

A possible additional validation is to input the SAGE-derived cloud information into an accurate radiative transfer model and to compare the calculated radiance / flux field at the top of the atmosphere with available satellite measurements (such as CERES). This kind of procedure has already become possible with the ISCCP and ERBE data sets [Rossow and Zhang, 1995]. The comparisons have proved to be useful indicators of the quality of information generated by the satellite retrievals.

Polar Stratospheric Clouds

Comparisons of SAGE III PSC observations should be made with any available PSC measurements of opportunity. Spaceborne solar occultation observations may be available from POAM II (or a follow-on) and ILAS, and spaceborne lidar measurements, such as from the LaRC-proposed PICASSO (Pathfinder Instruments for Cloud and Aerosol Spaceborne Observations platform, would be especially useful for detailed interpretation of the data. Comparisons should also be made with ground-based observations of PSCs from the Antarctic (Dumont d'Urville, McMurdo, Syowa) and the Arctic (Spitsbergen, Sodankyla, Andoya, Kiruna, Eureka).

3.10 Quality Control and Diagnostics

Quality control will have two components: an immediate "quick look" plan to indicate general data reliability and a monthly evaluation to assess data quality and to reset the uncertainty indices, if necessary, prior to data archival and release (see Section 3.6.2 for a summary of the complete data processing sequence). There is also a longer term validation plan for a more intense data quality scrutiny which is discussed in Section 3.9. In all the studies described below, compatibility with previous behaviour will be an important consideration.

Quick look quality control will consist of data screening to see if the data conforms to certain expected criteria. Control studies, which still have to be specified, might include examination of the following:

- Do the extinction values and their ratios fall within specified ranges?
- Are the signal termination altitudes reasonable i.e., close to or below the tropopause, except for PSCs?
- Do profiles for consecutive events resemble one another in terms of their gross features? This particular quality control filter will need careful specification as cloud is not likely to be correlated.

It may also be possible as part of the quick look screening to compare cloud presence or absence with the relative humidity derived for the same event (see Section 3.2.4 of the Solar and Lunar ATBD for details). Cloud may be expected to be associated with higher relative humidities. Use of this criterion is still tentative, as the water vapor data may not be available where cloud is present, and sharp vertical gradients in humidity may occur,

which will confuse any intercomparison. Comparison may also be possible with the temperature profile for the same event (see the SAGE III Solar and Lunar ATBD, Section 3.2.5 for details). In particular, it may be useful to compare the cloud altitude with that of the tropopause and to note any unusual behaviour.

The monthly quality control procedure will involve the generation of cloud cover latitude versus altitude profile maps, and latitude versus longitude distributions at standard altitude (each km) and/or standard pressure levels (300, 200, 150, 100, 70, 50, 30 hPa). Such maps are available from other data sources: the International Satellite Cloud Climatology Project (ISCCP), [Rossow and Garder, 1993a, 1993b], the High Resolution Infrared Sounder (HIRS) [Wylie and Menzel 1991; Wylie *et al*., 1994]; for high clouds from SAGE II [Liao *et al*., 1995a, 1995b], and from surface observations (see Rossow *et al*., 1993 for a review). The SAGE III cloud retrievals may be compared with climatological averages from other data sources as well as previous SAGE III data. Again, deviations from expectations will signal the need for further investigation, recognizing that differences may arise due to the limited data quantity and restricted diurnal sampling in the SAGE III data.

The utility of the cloud generation algorithm relies upon the validity of the aerosol retrieval and the nature of the aerosol present in the atmosphere. It will be useful to assess the quality and behaviour of the input aerosol data beyond that carried out for each event in the course of processing. In which case we will integrate data on a monthly basis and generate a series of monthly average latitude versus altitude profile maps, and latitude versus longitude distributions at standard altitude or pressure levels. Maps would be generated for the average extinction value and its error for each aerosol measurement (385, 448, 521, 595, 676, 757, 869, 1020, and 1540 nm) and for the ratios between extinctions at 521 and 1020 nm, and between 1020 and 1540 nm. Examination of such maps would be carried out in conjunction with any information about recent volcanic eruptions that may have injected material into the stratosphere. In times of non-volcanic activity, and at altitudes above the lower troposphere, little month to month variation is expected. Features that are attributable to recent eruptions should be readily visible at stratospheric altitudes and can be monitored to follow the dispersion of volcanic material and its subsequent loss from the stratosphere. Such features will also be visible to a somewhat lesser extent in the cloud occurrence maps, whose accuracy can then be assessed.

The time needed to carry out the quality assessment just described is presently undecided, but is likely to be between one week and one month. The assessment will be used as a basis for revising the cloud uncertainty indices at each altitude (see Section 3.5.1) for each event during the month under scrutiny. A monthly quality control instruction file will be generated containing the information necessary for revision of these indices. The detailed structure of this file still has to be decided; in view of the fact that much of the time there should be no revision needed (apart from the quality control flags), the file could have a hierarchical structure. In this, the main header would list the dates on which changes are to be made. Subheaders would exist for each date listed, showing in turn the event times for which changes are to be made. Finally, for each event listed, the altitudes

for which changes are necessary are given, together with the changes themselves. Following revision of the uncertainty indices, the quality assessment indices for all events (initially set to zero) are reset and the data archived. The flow chart for this operation is shown in Figure 3.10.1.
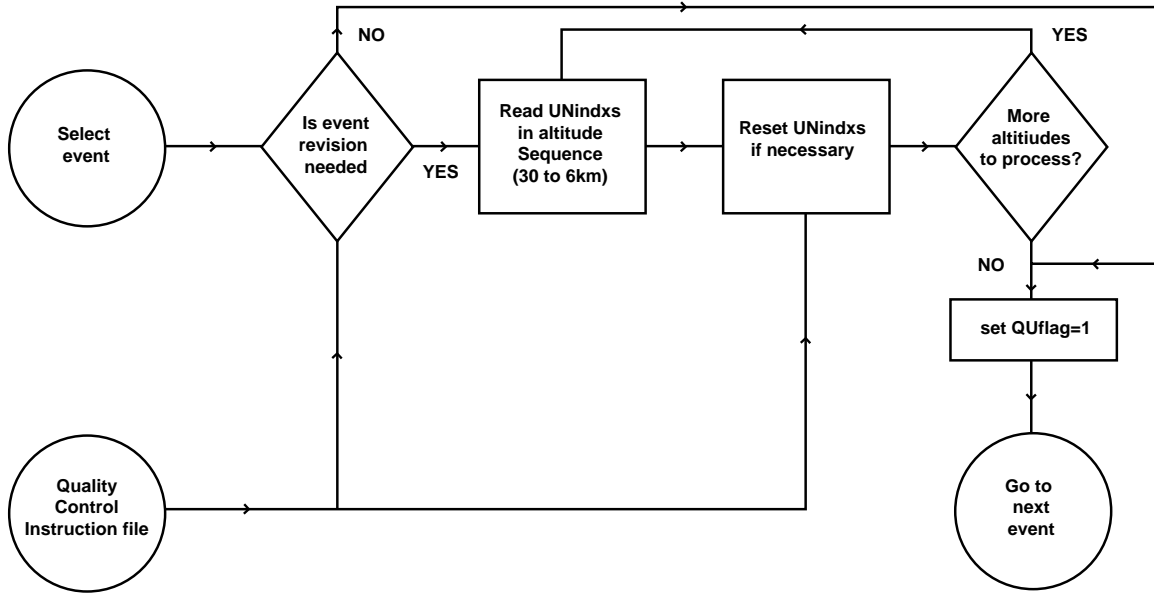
Figure 3.10.1 Flow chart for quality assessment and quality uncertainty index adjustment.

3.11 Exception Handling

The possible occurrence of exceptions to the data set must be anticipated and action devised to meet this. Exceptions may take the form of anomalous data whose source is not yet determined or of partial failure of the instrument so that some data are entirely missing or distorted. It is necessary first to recognize that a problem exists and second to take appropriate action to correct it or, if this is not possible, to switch to an alternative processing procedure.

Determination of cloud presence is a higher level procedure and requires processed multichannel aerosol data as input. It is anticipated that screening of the data for anomalies will be an integral part of the processing to aerosol extinction as described in the Solar and Lunar Algorithm ATBD. Here we are concerned with recognition of anomalies that might survive earlier screening and necessary action contingent on anomalies discovered at any stage of the analysis. Examples of anomalies that might be detected during the data inversion to aerosol extinction are missing data, either at all or at some wavelengths only; detected signals lying outside the expected signal ranges; and improper operation of the scanning cycle

Anomalies that might survive earlier processing but be detected during the determination of cloud presence might include improper ratios for extinction at the three wavelengths used, e.g.; systematic higher cloud extinction at 1540 nm than at 1020 nm; or signal termination at longer wavelengths occurring at greater altitudes than at the shorter wavelengths. These latter anomalies are likely to be detected as a result of the data validation and quality control procedures.

Appropriate action to be taken in the case of exception identification might consist of the following: (1) Either cessation of cloud processing for the anomalous event or events, or continuation of processing with the addition of an anomaly tag (this could simply be a special value of the quality assessment flag); (2) Examination of the cause of the anomaly and determination of options; (3) Re-analysis if the fault is correctable, or use of an alternative cloud presence determination strategy if the fault is not correctable. An example of the latter might be the total absence of data at one wavelength, e.g., 1540 nm. In such a case the fallback strategy might be to use a cloud inversion scheme based on two wavelengths only, such as was used for SAGE II data.

3.12 Possible Future Modifications

The present algorithm represents the best of the currently known cloud presence algorithms that have been examined in any detail. Other SAGE and SAGE II methods, not yet well explored, were briefly mentioned in Section 2.3. The availability of other SAGE III aerosol wavelengths presents further possibilities. It is anticipated that some of these alternatives will be explored and may lead to further algorithm development. Those possibilities that presently appear to merit further attention are listed below, together with some of the other potential high level developments that have been mentioned in the preceding text.

- Use of SAGE III aerosol wavelengths between 521 nm and 1020 nm. While use of these wavelengths is not likely to improve aerosol / cloud discrimination above 6 km altitude, they may prove very useful below that altitude.
- Incorporation of an additional criterion that depends upon the extinction amplitude or the vertical extinction gradient. Cloud leads to greater extinction values and to large vertical extinction gradients. Fresh volcanic aerosol and lofted tropospheric aerosol layers do the same but some distinction may very well exist.
- Improved simulations that include realistic error bars on the aerosol extinction values passed from the previous inversion. Such error bars will increase in magnitude in the presence of cloud due to the inhomogeneous nature of the clouds.
- Quality control procedures, as described earlier (Section 3.10), are mainly concerned with the identification of cloud data that is contaminated by unusually high aerosol loading, although other anomalies will be identified. It is anticipated that, at times, data may be anomalous and that the reasons for the anomaly will not be clear. Further work is required to specify what we consider to be anomalous data and how it should be identified in the output data (e.g., by another value of the uncertainty index). An

associated factor not yet included in the algorithm is that we may expect to receive some indication of data quality with the input extinction values (this may include engineering data anomalies as well). In what form this will arrive, and how it should be included into the cloud processing has yet to be defined.

- Use of SAGE III transmission profiles from individual scans across the sun rather than the extinction profiles which are based upon transmission profile averages. The raw transmission profiles contain information on inhomogeneities and extinction gradients, that may be lost in the data inversion. This information is potentially exploitable (see Appendix B).

- Use of lunar data. This data which will only exist above 15 km is not now being considered for the determination of cloud presence. It is potentially valuable to the identification and study of PSCs.

- Identification of PMCs. These have been mentioned as a possible future higher level data product. As information becomes available on these clouds from other sources, it may prove feasible to design a new sub-algorithm to detect them as part of the routine processing sequence.

- Inclusion of topographic data. Aerosol profiles will, in the absence of cloud, terminate at the earth's surface. This termination may be interpreted as opaque cloud, particularly if it occurs at a high elevation. Reference to a surface altitude database as each event is processed would help reduce the possibility of an incorrect determination of cloud presence. In is anticipated that this information may be included into the data stream at an earlier stage of the inversion.

4.0 Constraints, Limitations, Assumptions

Constraints

Due to the need for a quality control assessment, cloud data will not be available for archival or public release at the time of main processing. Data will be released in monthly blocks with a time delay of one week to one month from the end of the data block being released.

Limitations

The present algorithm will only operate between altitudes of 6 and 30 km. It will not be possible to identify the presence of cloud when large aerosols are present such as might be produced by volcanic injection or lofting of surface dust.

Assumptions

- Inverted aerosol extinction profiles at 521, 1020, and 1540 nm and their associated error bars and covariance will be available for each event with a vertical resolution of 0.5 km.

- The aerosol extinction values are uncontaminated by extinction due to any other atmospheric constituent.

- Cloud particles show little or no variation of extinction with wavelength.

- Aerosols show a distinctive variation of extinction with wavelength.

- Time periods (or individual occasions) during which aerosol extinction does not vary significantly with wavelength will be identifiable through either inspection of the data set or from external information on volcanic effects and general climatological information.

- Cloud inhomogeneity will not affect the determination process.

5.0 References

Barton, I. J., Upper level cloud climatology from an orbiting satellite, *J. Atmos. Sci.*, 40, 435-447, 1983.

Chiou, E. W., M. P. McCormick, W. P. Chu, and G. K. Yue; Distributions of cirrus determined from SAGE II occultation measurements between November 1984 and October 1988. Paper presented at Conference on Cloud Physics. *Amer. Meteor. Soc.,* San Francisco, July 23-27, 1990.

Debrestian, D.J., J. D. Lumpe, E. P. Shettle, R. M. Bevilacqua, J. J. Olivero, J. S. Hornstein, W. Glaccum, D. W. Rusch, and M. D. Fromm, Preliminary analysis of Southern Hemisphere POAM II observations of polar mesospheric clouds, *J. Geophys. Res.,* 102, 1971-1981, 1997a.

Debrestian, D., J. Lumpe, R. M. Bevilacqua, E. P. Shettle, J. S. Hornstein, and J. J. Olivero, POAM II observations of polar mesospheric clouds in the Southern Hemisphere, *Adv. Space Res.,* 19, 587-590, 1997b.

Deshler, T., B. J. Johnson, and W. R. Rozier, Balloonborne measurements of Pinatubo aerosol during 1991 and 1992 at 41°N: vertical profiles, size distribution, and volatility, *J. Geophys. Res.*, 20, 1435-1438, 1993.

Detwiler, A., and V. Ramaswamy, Radiative heating profiles in simple cirrus cloud systems. *J. Atmos. Sci.,* 47, 2167-2176, 1990.

Donahue, T. M., B. Guenther, and J. E. Blamont, Noctilucent Clouds in Daytime: Circumpolar Particulate Layers Near the Summer Mesopause, *J. Atmos. Sci.*, 30, 515-517, 1972.

Gadsen, M., and W. Schröder, Noctilucent Clouds, Springer-Verlag, 1989.

Goodman, J., K. G. Snetsinger, R. F. Pueschel, G. Ferry, and S. Verma, Evolution of Pinatubo aerosol near 19 km altitude over western North America, *Geophys. Res. Lett.*, 21, 1129-1132, 1994.

Hahn, C. J., S. G. Warren, J. London, R. M. Chervin, and R. Jenne, Atlas of simultaneous occurrence of cloud types over the ocean, NCAR Tech. Note TN-201+STR, 212pp. [NTIS PB 83-152074], 1982

Kent, G. S., L. R. Poole, and M. P. McCormick, Characteristics of Arctic polar stratospheric clouds as measured by airborne lidar, *J. Atmos. Sci.*, 43, 2149-2161, 1986.

Kent, G. S., L. R. Poole, M. P. McCormick, S. K. Schaffner, W. H. Hunt, and M. T. Osborn, Optical backscatter characteristics of Arctic polar stratospheric clouds, *Geophys. Res. Lett.,* 17, 377-380, 1990.

Kent, G. S., and M. P. McCormick, Separation of cloud and aerosol in two-wavelength satellite occultation data, *Geophys. Res. Lett.* 18, 428-431, 1991.

Kent, G. S., D. M. Winker, M. T. Osborn and K. M. Skeens, A model for the separation of cloud and aerosol in SAGE II occultation data, *J. Geophys. Res.,* 98, 20725-20735, 1993.

Kent, G. S., P-H. Wang, and K. M. Skeens, SAGE II measurements of high altitude tropical cloud, Preprint volume of the *Fifth Symposium on Global Change Studies and the Symposium on Global Electrical Circuit,* Global Change, and the Meteorological Application of Lightning Information, January 23-28, 1994, Nashville, TN Amer. Meteor. Soc., Boston, 1994.

Kent, G. S., E. R. Williams, P-H. Wang, M. P. McCormick and K. M. Skeens, Surface temperature related variations in tropical cirrus cloud as measured by SAGE II, *J. Climate*, 8, 2577-2594, 1995.

Kent, G. S., D. M. Winker, M. A. Vaughan, P-H. Wang, and K. M. Skeens, Simulation of SAGE II cloud measurements using airborne lidar data. *J. Geophys. Res*., 102, 21,795-21,807, 1997a.

Kent, G. S., P-H. Wang, and K. M. Skeens, Discrimination of cloud and aerosol in the Stratospheric Aerosol and Gas Experiment (SAGE III) occultation data, *Appl.Opt*., 33, 8639-8649, 1997b.

Knollenberg, R. G., and Huffman, D., Measurements of the aerosol size distribution in the El Chichon cloud, *Geophys. Res. Lett*., 10, 1025-1028, 1983

Liao, X., W. B. Rossow and D. Rind, Comparisons between SAGE II and ISCCP high-level clouds. Part I: Global and zonal mean cloud amounts. *J. Geophys. Res*., 100, 1121-1136, 1995a.

Liao, X., W. B. Rossow, and D. Rind, Comparisons between SAGE II and ISCCP high-level clouds. Part II: Locating cloud tops. *J. Geophys. Res*., 100, 1137-1148, 1995b.

Mauldin, L. E., Stratospheric Aerosol and Gas Experiment II instrument: a functional description, *Opt. Eng*., 24, 2, 307-312, 1985.

Mauldin, L. E., M. P. McCormick, J. M. Zawodny, L. R. McMaster, W. P. Chu, J. C. Gustafson, and G. L. Maddrea, The Stratospheric Aerosol and Gas Experiment III

instrument proposed for EOS: a conceptual design, *Int. Congress on Opt. Sci. and Eng.* - Paris, France, 1989.

McCormick, M. P., P. Hamill, T. J. Pepin, W. P. Chu, T. J. Swissler, and L. R. McMaster, Satellite studies of the stratospheric aerosol, *Bull. of the Amer. Met. Soc.*, 60, 9, 1979.

McCormick, M. P., W. P. Chu, G. W. Grams, P. Hamill, B. M. Herman, L. R. McMaster, T. J. Pepin, P. B. Russell, H. M. Steele, and T. J. Swissler, High-latitude stratospheric aerosol measured by SAM II satellite system in 1978-1979, *Science*, 214, 328-331, October, 1981.

McCormick, M. P., H. M. Steele, P. Hamill, W. P. Chu, T. J. Swissler, Polar stratospheric cloud sightings by SAM II, *J. Atmos. Sci.*, 39, 1387-1397, 1982.

McCormick, M. P., and C. R. Trepte, SAM II measurements of Antarctic PSCs and aerosols, *Geophys. Res. Lett.,* 13, 1276-1279, 1986.

McCormick, M. P., and C. R. Trepte, Polar stratospheric optical depth observed between 1978 and 1985, *J. Geophys. Res.*, 92, 4297-4306, 1987a.

McCormick, M. P., SAGE II: an overview, *Adv. Space Res.*, 7, 3, (3) 219-(3) 226, 1987b.

McCormick, M. P., G. S. Kent, W. H. Hunt, M. T. Osborn, L. R. Poole, and M. C. Pitts, Arctic polar stratospheric cloud observations by airborne lidar*, Geophys. Res. Lett.*, 17, 381-383, 1990.

McCormick *et al*., Stratospheric Aerosol and Gas Experiment III (SAGE III) Aerosol and trace gas measurements from Earth Observing System (EOS), SPIE Paper No. 1491-16, *SPIE Symposium on Aerospace Sensing*, Orlando, Florida, 1991.

McCormick, M.P., and R. E. Veiga, SAGE II measurements of early Pinatubo aerosols, *Geophys. Res. Lett.*, 19, 155-158, 1992.

McCormick, M. P., J. M. Zawodny, W. P. Chu, J. W. Baer, J. Guy, and A. Ray, Stratospheric Aerosol and Gas Experiment III (SAGE III), *SPIE International Symposium for Optical Engineering* - Orlando, FL, 1993a.

McCormick, M. P., D. M. Winker, E. V. Browell, J. A. Coakley, C. S. Gardner, R. M. Hoff, G. S. Kent, S. H. Melfi, R. T. Menzies, C. M. R. Platt, D. A. Randall, and J. A. Reagan, Scientific investigations planned for the Lidar In-Space Technology Experiment (LITE), *Bull. Amer. Meteor. Soc.*, 74, 205-214, 1993b.

Olivero, J. J. and G. E. Thomas, Climatology of polar mesospheric clouds, *J. Atmos. Sci.,* 43, 1263-1274, 1986.

Oberbeck, V. R., E. F. Danielsen, K. G. Snetsinger, and G. V. Ferry, Effect of the eruption of El Chichon on stratospheric aerosol size and composition, *Geophys. Res. Lett.,* 10, 1021-1024, 1983.

Osborn, M. T., L. R. Poole, and P.-H. Wang, SAM II and lidar aerosol profile comparisons During AASE, *Geophys. Res. Lett.,* 17, 401-404, 1990.

Pepin, T. J. and M. P. McCormick, Stratospheric Aerosol Measurement Experiment MA-007, NASA TM X-58173, February, 1976

Poole, L. R., and M. P. McCormick, Airborne lidar observations of Arctic polar stratospheric clouds: Indications of two distinct growth stages*, Geophys. Res. Lett*., 15, 21-23, 1988.

Poole, L. R., M. T. Osborn, and W. T. Hunt, Lidar observations of Arctic polar stratospheric clouds: Signature of small, solid particles above the frost point, *Geophys. Res. Lett.,* 15, 867-870, 1988.

Poole, L. R., G. S. Kent, M. P. McCormick, W. H. Hunt, M. T. Osborn, S. K. Schaffner, and M. C. Pitts, Dual-polarization airborne lidar observations of polar stratospheric cloud evolution*, Geophys. Res. Lett.,* 17, 389-392, 1990.

Poole, L. R., and M. C. Pitts, Polar stratospheric cloud climatology based on Stratospheric Aerosol Measurement II observations from 1978-1989, *J. Geophys. Res.,* 99, 13,083-13,089, 1994.

Pueschel, R. F., S. A. Kinne, P. B. Russell, K. G. Snetsinger, and J. M. Livingstone, Effects of the 1991 Pinatubo volcanic eruption on the physical and radiative properties of stratospheric aerosols, in *IRS '92: Current Problems in Atmospheric Radiation*, Eds. S. Keevallik, and O. Kärner, pp 183-186, A. Deepak Publishing, Hampton, Virginia, 1993.

Pueschel, R. F., P. B. Russell, D. A. Allen, G. V. Ferry, K. G. Snetsinger, and J. M. Livingston, Physical and optical properties of the Pinatubo volcanic aerosol: aircraft observations with impactors and a Sun-tracking photometer, *J. Geophys. Res*., 99, 12915-12922, 1994.

Ramanathan, V., E. J. Pitcher, R. C. Malone, and M. L. Blackmon, The response of a general circulation model to refinements in radiative processes. *J. Atmos. Sci*., 40, 605-630, 1983.

Ramaswamy, V., and V. Ramanathan, Solar absorption by cirrus clouds and the maintenance of the tropical upper troposphere thermal structure. *J. Atmos. Sci*., 47, 2167-2176, 1989.

Rossow, W. B. and L. C. Garder, Cloud detection using satellite measurements of infrared and visible radiances for ISCCP. *J. Climate*, 6, 2341-2369, 1993a.

Rossow, W. B. and L. C. Garder, Validation of ISCCP cloud detections. *J. Climate*, 6, 2370-2393, 1993b.

Rossow, W. B., A. W. Walker, and L. C. Garder, Comparison of ISCCP and other cloud amounts. *J. Climate*, 6, 2394-2418, 1993.

Rossow, W. B., and Y-C. Zhang, Calculation of surface and top of atmosphere radiative fluxes from physical quantities based on ISCCP data sets, 2, Validation and first results. *J. Geophys. Res*., 100, 1167-1197, 1995.

Rusch, D. W., G. E. Thomas, and E. J. Jensen, Particle size distributions in Polar mesospheric clouds derived from solar mesospheric explorer measurements, *J. Geophys. Res*., 96, 12933-12939, 1991.

Sassen, K. and B. S. Cho, Subvisual-thin cirrus lidar dataset for satellite verification and climatological research, *J. Appl. Meteor*., 31, 1275-1285, 1992.

Sassen, K., M. K. Griffin and G. C. Dodd, Optical scattering and microphysical properties of subvisual cirrus clouds, and climatic implications, *J. Appl. Meteor*. 28, 91-98, 1989.

Schreiber, H. G., M. Wirth, and W. Renger, Airborne backscatter lidar meaurements of the DLR-ALEX during ELITE. Paper presented at the *AGU Spring Meeting,*May30-June2, Baltimore, Maryland, 1995.

Shettle, E. P., M. D. Fromm, D. Debrestian, J. S. Hornstein, K. W. Hoppel, J. Lumpe, W. J. Glaccum, J. J. Olivero, R. M. Bevilacqua, and S. S. Krigman, Observations of clouds in the polar stratosphere and polar mesosphere from POAM II, *SPIE Proceedings*, 2578, 138-145, 1995.

Smith, W. L. and C. M. R. Platt, Intercomparison of radiosonde, ground based laser, and satellite deduced cloud heights. *J. Appl. Meteor*., 17, 1796-1802, 1978.

Snetsinger, K. G., R. F. Pueschel, and G. V. Ferry, Diminished effects of El Chichon on stratospheric aerosols, early 1984 to late 1986, *Atmos. Environ*., 26A, 2947-2951, 1992.

Stanford, J. L., and J. S. Davis, A century of stratospheric cloud reports: 1870-1972, *Tellus*, 29, 530-534, 1974.

Stowe, L. L., H. Y. M. Yeh, T. F. Eck, C. G. Wellemeyer, and H. L. Kyle, Nimbus-7 global cloud climatology. Part II: First year results, *J. Climate*, 2, 671-709, 1989.

Thomas, G. E., Mesopause clouds and the Physics of the Mesopause Region, *Rev. Geophys.*, 29, 553, 1989.

Thomas, G. E. and J. J. Olivero, Climatology of polar mesospheric clouds, 2. Further analysis of solar mesospheric explorer data, *J. Geophys*. *Res*., 94,673-14,702, 1989.

Wang, P-H., M. P. McCormick, L. R. Poole, W. P. Chu, G. K. Yue, G. S. Kent, and K. M. Skeens, Tropical high cloud characteristics derived from SAGE II extinction measurements, *Atmos. Res*. 34, 53-83, 1994.

Wang, P-H.. M. P. McCormick, P. Minnis, G. S. Kent, G. K. Yue, and K. M. Skeens, A method for estimating the vertical distribution of the SAGE II opaque cloud frequency, *Geophys. Res. Lett*., 22, 243-246, 1995.

Wetherald, R., V. Ramaswamy, and S. Manabe, A comparative study of the observations of high clouds and simulations by an atmospheric general circulation model. *Clim. Dyn.*, 5, 135-143, 1991

Wilson, J. C., H. H. Jonsson, C. A. Brock, D. W. Toohey, L. M. Avallone, D. Baumgardner, J. E. Dye, L. R. Poole, D. C. Woods, R. J. DeCoursey, M. Osborn, M. C. Pitts, K. K. Kelly, K. R. Chan, G. V. Ferry, M. Loewenstein, J. R. Podolske, and A. Weaver, In situ observations of aerosol and chlorine monoxide after the eruption of Mount Pinatubo: effects of reactions on sulfate aerosol, *Science*, 261, 1140-1143, 1993.

Woodbury, G. E. and M. P. McCormick, Global distributions of cirrus clouds determined from SAGE data, *Geophys. Res. Lett.,* 10, 1180-1183, 1983.

Woodbury, G. E., and M. P. McCormick, Zonal and geographical distribution of cirrus clouds determined from SAGE data, *J. Geophys. Res*., 91, 2775-2785, 1986.

Wylie, D. P., and W. P. Menzel, A cirrus cloud climatology from NOAA/HIRS. Paleoclimatol. Paleoecol. (Global Planet. Change Sect.), 90, 49-53, 1991.

Wylie, D. P., W. P. Menzel, H. M. Woolf and K. I. Strabala, Four years of global cirrus cloud statistics using HIRS. *J. Climate* (submitted, 1994)

Appendix A. SAGE III Instrument Description

The design of the SAGE III sensor relies heavily upon the flight proven designs used in the SAM II and SAGE I/II instruments. Specifically, the separate sensor and electronics modules concept from SAGE II is utilized, as are the grommet isolation and contamination door designs. Additionally, the SAGE II pointing system and scan mirror designs are reused, with certain necessary modifications (primarily an attenuator filter) to permit solar and lunar observations with the same detector assembly.

The SAGE III sensor assembly, illustrated in Figure A.1, consists of a sun-tracker, telescope, and grating spectrometer with a CCD detector array; the mass is estimated at 35 kg., a volume of 6000 cm^3, with an average power of 60 W and a peak power of 75 W. The two-axis passive sun-tracker, with a scan mirror that scans the instrumental field of view across the solar disk, obtains multiple samples at each altitude, improving the measurement precision. Sunspots are readily detected by scanning, rather than staring at the Sun. A pictorial representation of the scanning pattern as a function of tangent altitude and the corresponding detector output (single wavelength) is illustrated in Figure A.2. The two solid lines denote the position of the top and bottom of the solar disk during a sunrise event as viewed from the spacecraft. The gradual expansion of the vertical sun shape is due to atmospheric refraction. The ordinate denotes the tangent altitude, while the abscissa denotes the event time. During an occultation event, the instrument scans the solar disk as indicated by the dashed line in the figure.

The telescope and spectrometer are illustrated in Figure A.3 and constitute new designs optimized to meet the requirements of lunar occultation measurements. The telescope is a f/4 Dall-Kirkham configured design chosen for its ease of alignment; the speed represents a tradeoff between optimum performance and spectral imaging. The spectrometer is a new design, utilizing a holographic, aberration reduced, grating to provide stigmatic imaging at 440 and 868 nm with 1 nm resolution below 450 nm and 2 nm resolution between 740 and 960 nm. The grating is formed on a spherical substrate with a radius of 152 mm and is imaged through a field flattener and order-sorting filters onto the CCD detector. The grating is utilized in the first positive order with diffraction angles between 8.3 and 17.0 degrees; a ruling of 199 lines per millimeter yields a dispersion of 0.94 to 1.88 nm per pixel in the focal plane (depending on wavelength). Evaluation gratings have been tested and demonstrate near-theoretical first-order efficiencies with very low scattered light properties. The spectrometer has been ray-traced and a Monte Carlo simulation of optical tolerances has been performed which indicates that at the wavelengths of best spectral focus, a FWHM bandpass of less than 1.2 nm per pixel should be achievable.

The detector assembly consists of two elements, a Tektronix 809x10 pixel backside-illuminated, thinned CCD array for the 280 - 1040 nm spectral region and a InGaAs infrared photodiode (1550 ± 15 nm) that are spatially co-registered. The 809 elements of the array provide the spectral information, the 10 pixels aligned along the horizontal direction are summed together and can be considered a single long pixel. Practical

considerations favor pixel subdivision: large pixels can have a low charge transfer efficiency which can be avoided through subdivision, and secondly reducing the horizontal instantaneous field of view (IFOV) can improve the probability of cloud-free measurements. Consequently, in the solar occultation mode, 3 pixels (0.5x1.5 arcminute IFOV) are used to improve the frequency of penetration of the measurements into the troposphere. In contrast, for the lunar occultation measurements, all 10 pixels are used to collect more light.

In the solar occultation mode, the optical throughput of the instrument (grating efficiency and CCD quantum efficiency) combined with the spectral variation in the solar spectrum produce a wide variation in the rate of charge accumulation in the CCD pixels as a function of wavelength. Optimum performance (signal-to-noise ratio and dynamic range) of the detector is achieved when pixels are operated at or near full well. To obtain full well across the spectral region, a spectral flattening filter was considered to selectively attenuate the spectrum near the middle of the spectral band pass, but was determined to be too difficult to design. Instead, the array has been divided into eight segments that have individually controlled integration times to control the filling of the wells. Each segment is operated at or near full well, and the transitions between segments are chosen to avoid potential science channels. This solution optimizes performance and eliminates an item of significant risk and cost.

The lunar occultation measurements are significantly more complicated than the solar measurements; depending upon phase, the Moon is between one million and ten million times less luminous than the Sun, and the lunar albedo is non-uniform making determination of atmospheric transmission non-trivial. The instrument is designed to compensate for this large change in illumination in part by removing the solar attenuator (a neutral density filter with an attenuation of 100) from the optical path. In addition, the integration time is increased from 0.09-2.2 milliseconds to 62 milliseconds (with a resulting increase in signal of 28 to 500), and the instrumental field of view is increased from 3 pixels to 10 pixels (producing an increase of 3.3 in signal level). The resulting gain increase of 165,000 should permit lunar measurements with a signal-to-noise ratio of 150-300, only a factor of 10-20 times poorer than the solar measurements which implies that the altitude range for the species retrievals will be somewhat reduced in the lunar occultation mode.

The detector package has been modeled and electrical, optical, thermal, and radiation-shielding testing of prototype detectors has been performed. The detector assembly is surrounded by an aluminum radiation shield (nominally 1-inch thick) and is illustrated in Figure A.4. The housing is comprised of a base plate, a lead frame assembly, and an optical field flattener. The lead frame assembly is an insulating rectangle through which the electrical connections to the detector and a thermoelectric cooler (TEC) pass. The field flattener is a plano-concave sapphire window. The purpose of the field flattener, in addition to providing a window to the sealed CCD package, is to further increase the radius of curvature of the focal field and coincide better with the planar CCD array.

Mounted to the backside of the field flattener are three order-sorting filters that provide the out-of-band rejection of light diffracted towards the focal plane assembly from other grating orders. The CCD is mounted to a TEC that is, in turn, mounted to the base plate heat sink. The CCD is designed with built-in thermistors that are part of an active temperature control system to meet the stability and end-of-life dark current requirements. The detector assembly has been included in the stray light analysis of the spectrometer, which showed that a significant reduction in the amount of scattered light could be achieved by rotating the CCD about its long axis by 11 degrees and eliminating internal reflections within the detector assembly. Also within the detector assembly is the InGaAs photodiode for the 1540 nm channel. This channel lies in the zero-order beam and has its band pass determined by a filter in much the same manner as was done with two of the channels in SAGE II. This detector is within the assembly because of the close proximity of the zero-order light rays to the end of the CCD array. Prototype detectors have been manufactured and tested for spectral quantum efficiency, dark current versus temperature, full-well capacity, charge transfer efficiency, and linearity. Radiation testing with monoenergetic proton beams of differing total doses have assessed the performance in a radiation environment, and led to models of energetic particle transport and secondary particle production, and an assessment of the shielding requirements for the CCD. In addition, models were developed to describe the observed temperature dependent gain of the field effect transistor preamplifiers on the CCD.

The spectrometer with the CCD array of detectors provides continuous wavelength coverage between 280 and 1040 nm and will permit the measurement of multiple absorption features of each gaseous species and multi-wavelength measurements of broadband extinction by aerosols. In the present configuration, 12 solar channels ($\leq$80 sub-channels) will be routinely utilized in the solar occultation measurements and 3 channels (340 sub-channels) in the lunar occultation measurements, greatly decreasing the random error in the measurements (precision), and allowing for more accurate modeling of the multi-wavelength aerosol extinction. Included within the instrument band pass is the O_2 A-band (around 760 nm) which will permit the retrieval of density and temperature with which the viewing geometry (as a pressure level) can be inferred. This improvement over SAGE II, which relied upon the NOAA gridded analyses, should improve the accuracy of the SAGE III profiles and simplify the comparison with other measurements. Additionally, the linear array of detectors will permit on-orbit wavelength and intensity calibration from observations of the exoatmospheric solar Fraunhofer spectrum. The continuous spectral calibration, combined with the self-calibrating nature of the occultation technique (ratioing the signal transmitted through the atmosphere to the exoatmospheric reference signal for each measurement) makes SAGE III ideal for long-term monitoring of trends in ozone and other gas species, which is a central objective of the EOS program.

The expanded spectral coverage of the SAGE III instrument permits the observation of O_3 in the mesosphere between 65 and 85 km by utilizing the UV absorption in the short wavelength region between 385 and 290 nm and, combined with a fixed channel InGaAs detector at 1550 nm, should greatly enhance the characterization of multi-wavelength aerosol and clouds and extend this capability to lower altitudes in the troposphere. The

CCD array will provide approximately 2-nm resolution in the spectral region between 920 and 960 nm. In combination with an increase in digitization from 12 bit precision to 16 bit precision, this should allow for greater discrimination of water vapor from aerosol (both volcanic and thin cloud), and better retrieval of the higher water vapor values at lower altitudes in the troposphere than was possible with SAGE II. Table A.1 details the measurement capability of SAGE III for single profile retrievals. The notable difference, as discussed above, is the determination of pressure and temperature from oxygen A-band and the improved precision from the inclusion of additional channels.

With a 16-bit A/D converter, the SAGE III spectrometer will allow for variable integration time and on-orbit gain programming necessary for lunar observations. This potentially doubles the number of measurements per orbit, but requires a detector and signal chain that can accommodate the reduced flux observed during lunar occultations. In lunar occultation SAGE III will monitor O_3, NO_2, pressure, and H_2O, as well as OClO and NO_3.

Table A.1: SAGE III measurement capability (single profile)

Channel	Wavelength (nm)	Products	Solar Altitude	Error (%)	Lunar Altitude (km)	Error (%)
S1	290	O_3	50-85	10	----	----
S2	385	Aerosol	15-40	10	----	----
L1	380-420	OClO	----	----	15-25	25
S3/L1	433-450	NO_2, Aerosol	10-50, 10-40	15 ----	20-50	10
L1	470-490	O_3	----	----	16-35	10
S4	521	Aerosol, Cloud	6-40	10 ----	----	----
S5	560-616	O_3	6-60	5	----	----
L1	640-680	NO_3	----	----	20-55	10
S6	670	Aerosol	3-40	5	----	----
S7	758	Aerosol	3-40	5	----	----
S8/L2	759-771	Pressure, Temperature	0-85, 0-85	2 2K	--------	---- ----
S9	869	Aerosol	0-40	5	----	----
S10/L3	933-960	H_2O,	0-50,	15	----	----
S11	1020	Aerosol, Cloud	0-40	5	----	----
S12	1540	Aerosol, Cloud	0-40	5	----	----

a. Error is estimated precision

b. Lowest altitude is determined by cloud top height
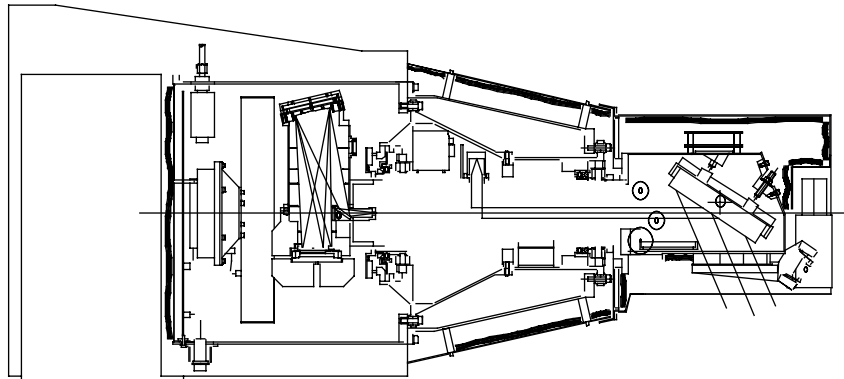
Figure A.1. The SAGE III sensor assembly.
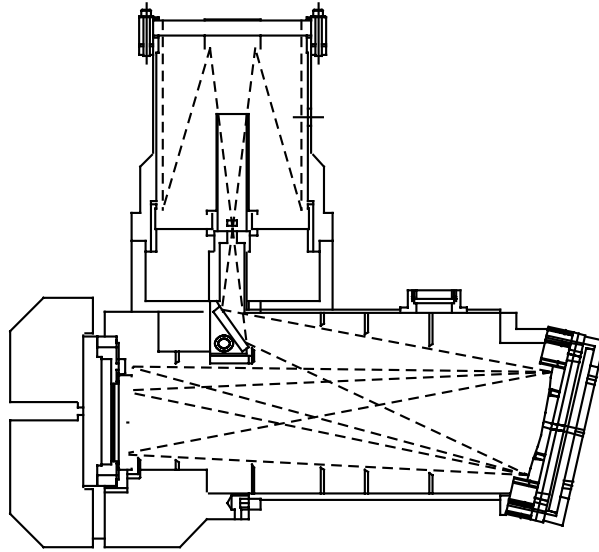
Figure A.2. Optical configuration and ray paths for the SAGE III telescope and spectrometer.

Side Section View
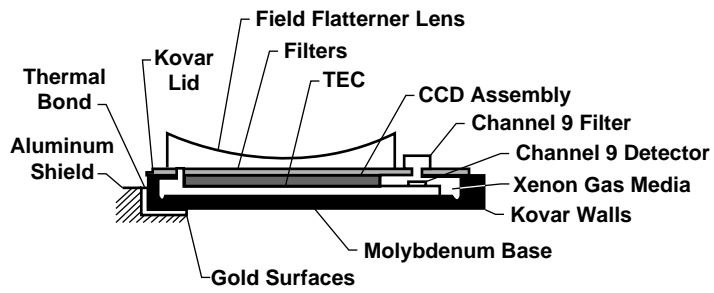
End Section View
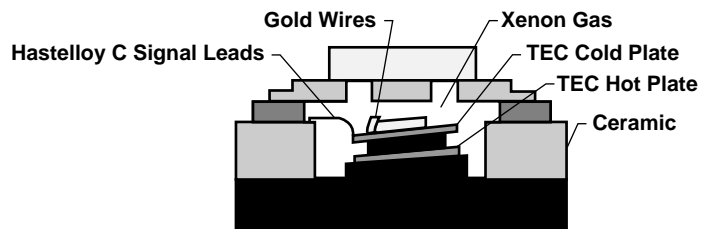
Figure A.3. SAGE III detector package.

Appendix B. Atmospheric Inhomogeneity

The SAGE III inversion algorithm, as do essentially all processing algorithms for limb viewing instruments, assumes that the atmosphere is spherically homogeneous. This is probably a good assumption for most stratospheric constituents but is not always true for cloud and may well be a poor approximation for other constituents in the troposphere. Of all the species measured by SAGE III, cloud is most likely to be affected by its own inhomogeneous nature. Despite this, the current SAGE III algorithm, essentially an extension of that used for SAGE II [Kent *et al*., 1993], neglects this feature of cloud observations. Simulation studies are in progress that may lead to modifications in the cloud detection algorithm that exploit inhomogeneity as a tool to infer the presence of cloud. Inhomogeneous cloud, whether stratospheric or tropospheric, is likely to degrade the quality of concurrent SAGE III measurements of molecular species and temperature and pressure.

Airborne lidar data, taken on an approximately 8000 km flight path over the tropical Pacific, has been used to simulate high altitude SAGE II cloud measurements and their inversion [Kent *et al.*, 1997a]. These simulations produce cloud extinction values similar in magnitude and distribution to those obtained from SAGE II. They also show the existence of three possible error conditions that result from the inhomogeneous nature of the cloud:

1) The true altitude of a cloud may be higher than that found as a result of the SAGE II inversion. Errors of 1 km or more occurred in ~40% of the data set.

2) The inverted cloud extinction may differ (biased low) from the volume averaged extinction along the horizontal ray path.

3) The presence of non-uniform or isolated cloud patches can result in an apparent negative inverted extinction value just below the cloud. Such values were observed in about one third of the simulations. The present SAGE II inversion scheme (bottom up Twomey-Chahine) suppresses these negative values but compensates by reducing the extinction value just above the offending level.

SAGE transmission measurements are an amalgamation of several independent scans across the sun. In the presence of cloud or other inhomogeneities, these scans will measure different amounts of transmitted radiation from the same point on the sun (because the spacecraft moves and the instrument line of sight at a given tangent altitude, as a result, also moves). These differences are manifested in the transmission data as an increased standard deviation relative to homogeneous conditions. The possibility exists that this variability may be used as a additional input to the cloud detection algorithm. The simulation described above has been extended to include spacecraft motion and compared to results from SAGE II observations.

Figure B.1 shows a scatter plot of SAGE II data at an altitude of 14.5 km in which the relative error in the slant path optical depth (SPOD) has been plotted against the SPOD

itself. Low values of SPOD, corresponding to cloud-free observations, show low relative error. As cloud is observed in some scans, the relative error increases to a maximum as SPOD also increases. Then as more and more scans observe cloud, the relative error decreases as SPOD continues to increase. Figure B.2 shows the equivalent simulation using airborne lidar data. The behavior is very similar to that shown in Figure B.1. Individual data points in this figure are coded by their wavelength extinction ratio (525 nm to 1020 nm aerosol extinction ratio). This ratio is used as the primary discriminator between cloud and aerosol in SAGE II observations and is similar to that proposed for the SAGE III algorithm. We note that the majority of the high error cases (mixed cloud) would be identified as cloud due to their low extinction ratio. However, some high error cases have higher extinction ratios and would not be identified as cloud by the SAGE II algorithm though cloud is clearly present.

Based on these results, we plan to carry out further simulations of the effect of cloud and other inhomogeneities on the inversion algorithm and data quality (not only on cloud presence but also for all other detected species). In particular, we will investigate the effects of PSCs on data from the SAGE III/Meteor 3M flight. The outcome of further simulations may lead to modifications of the inversion algorithm (particularly for cloud detection) and error estimation. We will also consider the implication of cloud homogeneity on the SAGE III validation program (particularly its tropospheric section).
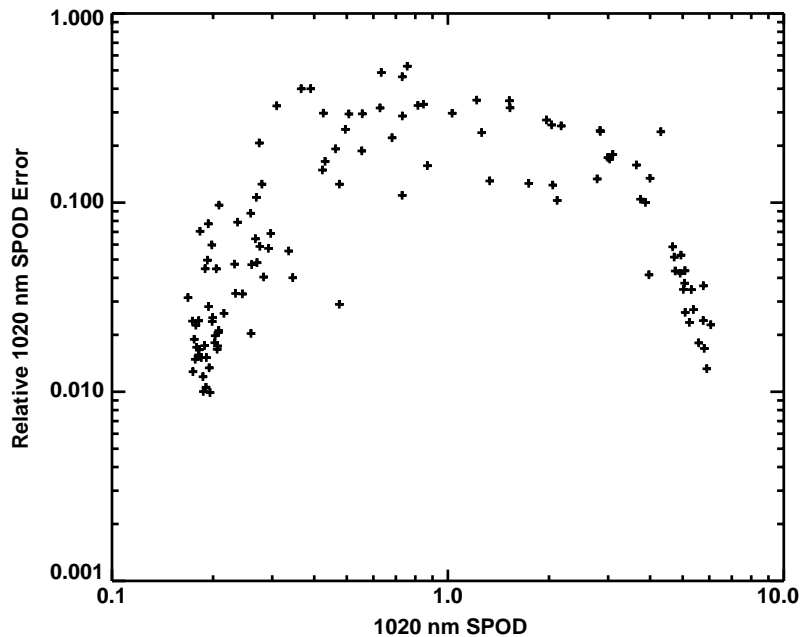
Figure B.1 A scatter plot of SAGE II data at an altitude of 14.5 km, in which the relative error in the slant path optical depth (SPOD) is plotted against the SPOD itself. Data points cover both cloudy and non-cloudy situations.
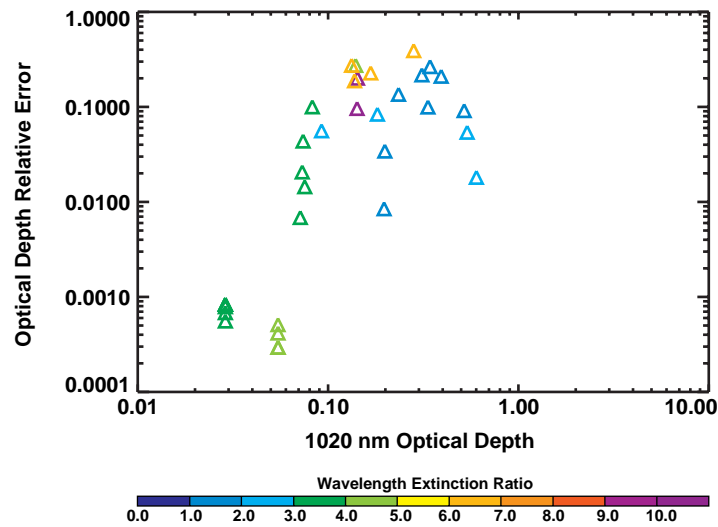
Figure B.2   Scatter plot equivalent to that shown in figure B.1, but derived from simulations based on airborne lidar data obtained within a cloud field. The color coding shows the retrieved 525 nm to 1020 nm aerosol extinction ratio.

References

Kent, G. S., D. M. Winker, M. T. Osborn and K. M. Skeens, A model for the separation of cloud and aerosol in SAGE II occultation data, *J. Geophys. Res.,* 98, 20725-20735, 1993.

Kent, G. S., D. M. Winker, M. A. Vaughan, P-H. Wang, and K. M. Skeens, Simulation of SAGE II cloud measurements using airborne lidar data. *J. Geophys. Res.*, 102, 21,795-21,807, 1997.

Appendix C A Possible 3-Dimensional Approach

This approach suggest is an extension of the 2-wavelength method of Kent *et al*. [1993], who intercompared data at 525 nm and 1020 nm and used the observed wavelength variation in extinction to distinguish aerosol from cloud. In the 3-D case we plot extinction data at 525 nm, 1020 nm and 1550 nm in 3-D space, and similarly use the differential wavelength behavior to separate the aerosol from the cloud. There is the potential advantage over the 3-wavelength method described in the ATBD that an extra parameter - the absolute value of the extinction - is available to assist in the aerosol-cloud separation. The method is illustrated in Figure C.1. In this figure the orange filled circles show data points derived from measured in situ stratospheric aerosol size distributions (105 separate measurements). They are the same data points as those used for the analysis presented in the ATBD; both background (11 measurements) and volcanically contaminated aerosol data (94 measurements) are represented here. The blue crosses in Fig 1 show the results of adding varying amounts of cloud, again the cloud conditions are the same as those described in the ATBD. The problem of separating aerosol from cloud becomes, in its simplest form, a search for a surface within this space that will divide the aerosol from the cloud data points. Following the 2-dimensional analysis of Kent *et al*. [1993], this search has so far been limited to plane surfaces.

Method of Search for a Suitable Dividing Plane

Data visualization in 3 dimensions is not simple and, in the present case, contouring or shading is not a suitable option. As an aid to visualization, the data points have been color coded, using a standard 3-color system, to show their location in space. An animated display has then been created in which the data cube (as in Figure C.1) is rotated to view the individual data points from differing perspectives. The special cases in which one wavelength is suppressed have also been examined, in order to ensure that the present analysis is compatible with 2-wavelength analyses previously made. It is clear from these studies that, as in the previous studies of alternative methods of distinguishing aerosol and cloud there is no method, using the present wavelength set, of achieving perfect separation of volcanic aerosol and cloud.

Potential dividing planes for separating the aerosol from the cloud have been defined in terms of their direction cosines and the perpendicular distance from the origin. The defining parameters have then been varied over a complete range of likely values, and the error rate for the separation of aerosol and cloud determined. The neighborhood of parameter values where the error rate was low have been studied in more detail in order to determine the optimum values for the defining parameters.

Results of the Search

The search method just described showed that, for a plane surface, the lowest error rate for aerosol-cloud separation under volcanic conditions was about 35%. This value is better than that achieved using any of the 2-wavelength methods (41% using 1020 nm/1550 nm and 65% using 525 nm/1020 nm) but not as good as that found using the 3-

wavelength method proposed in the ATBD (29%). The 3-D method also suffers from the disadvantage that different parameters must be used for the plane of separation according to the type of aerosol present. This feature is shared with the method now used for SAGE II data (525 nm/1020nm) but not the 3-wavelength method proposed in the ATBD.

Recommendation and Need for Future Work

Based on results so far obtained, the aerosol / cloud method proposed in the ATBD is superior to the 3-dimensional method described above so long as the latter is restricted to the use of plane surfaces for aerosol/cloud separation. It is possible that an investigation of higher order surfaces may yield a better solution. This will require better visualization techniques and computer software.
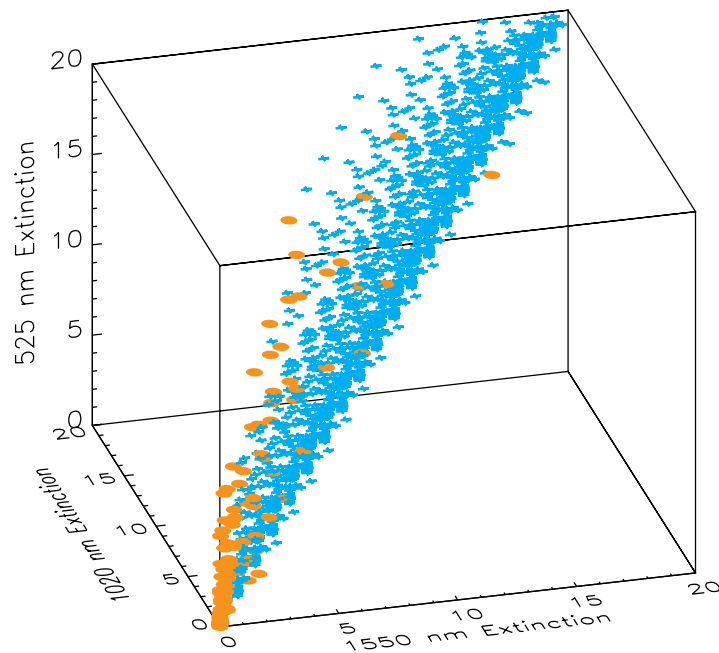
Figure C.1 3-dimensional scatter plot of simulated aerosol and cloud data. Orange - aerosol / blue - cloud.

References

Kent, G. S., D. M. Winker, M. T. Osborn and K. M. Skeens, A model for the separation of cloud and aerosol in SAGE II occultation data, *J. Geophys. Res.,* 98, 20725-20735, 1993.